USGS
science for a changing world

USGS Science Strategy to Support U.S. Fish and Wildlife Service Polar Bear Listing Decision

Uncertainty in Climate Model Projections of Arctic Sea Ice Decline: An Evaluation Relevant to Polar Bears

By Eric DeWeaver[1]

Administrative Report

U.S. Department of the Interior
U.S. Geological Survey

U.S. Department of the Interior
DIRK KEMPTHORNE, Secretary

U.S. Geological Survey
Mark D. Myers, Director

U.S. Geological Survey, Reston, Virginia: 2007

Author affiliation:

[1] Center for Climate Research, Atmospheric and Oceanic Sciences Department, University of Wisconsin – Madison

Contents

Figures

Abbreviations, Acronyms, and Symbols

Abbreviations, Acronyms, and Symbols	Meaning
20C3M	20th Century climate in coupled models
A1B	IPCC forcing scenario A1B
A2	IPCC forcing scenario A2
ACIA	Arctic Climate Impact Assessment
AO	Arctic Oscillation
AOGCM	Atmosphere-ocean general circulation model
AOMIP	Arctic Ocean Model Intercomparison Project
AR4	IPCC Fourth Assessment Report
AW	Atlantic water
B1	IPCC forcing scenario B1
CCMA_CGCM	Canadian Center for Climate Modeling and Analysis climate model
CCSM3	NCAR Community Climate System Model, version 3
CMIP	Coupled Model Intercomparison Project
CMIP2	Second CMIP
CHL	Cold Halocline Layer
EVP	Elastic-viscous-plastic
GCM	General Circulation Model
GFDL	Geophysical Fluid Dynamics Laboratory (U.S.)
GISS	Goddard Institute for Space Studies (U.S.0
GISS-ER	GISS climate model
HadCM3	Hadley Center for Climate Prediction and Research climate model
HadGEM1	Hadley Center for Climate Prediction and Research climate model
HadISST	Hadley Center Sea Ice and Sea Surface Temperature data set (Raynor et al. 2003)
IABP	International Arctic Buoy Program
IAP_FGOALS	Institute of Atmospheric Physics (China) climate model
INMCM	Institute for Numerical Mathematics (Russia) climate model
IPCC	Intergovernmental Panel on Climate Change
MRI-CGCM	Meteorological Research Institute (Japan) climate model
NAO	North Atlantic Oscillation

Abbreviations, Acronyms, and Symbols (continued)

Abbreviations, Acronyms, and Symbols	Meaning
NCAR	National Center for Atmospheric Research (U.S.)
NSIDC	National Snow and Ice Data Center (U.S.)
OHFC	Ocean heat flux convergence
SHEBA	Surface Heat Budget of the Arctic
TAR	IPCC Third Assessment Report
UKMO_HADGEM1	Hadley Center for Climate Prediction and Research climate model
USFWS	U.S. Fish and Wildlife Service
USGS	U.S. Geological Survey

Arctic Ocean Place Names

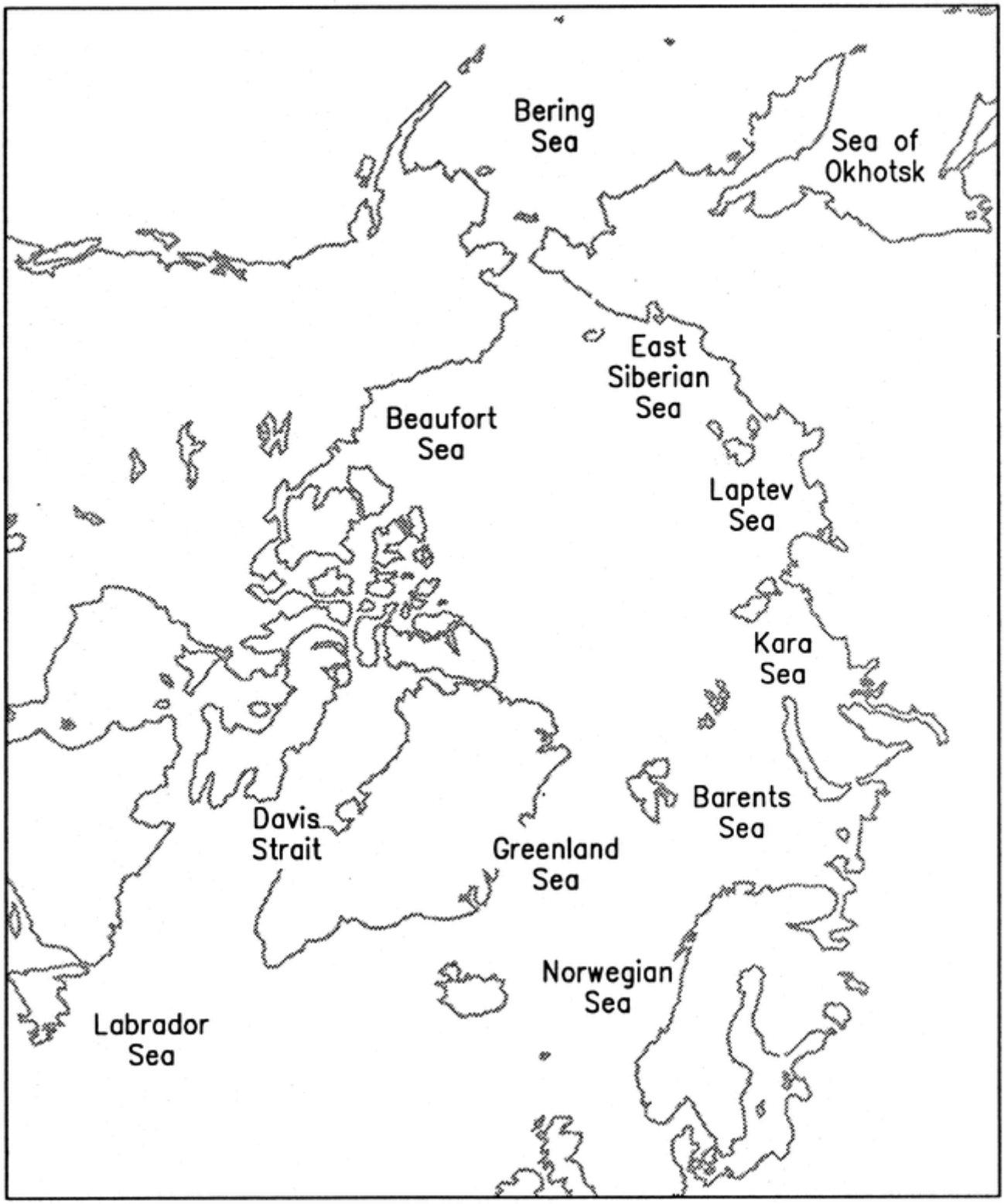

(From Deser and Timlin 2000)

Uncertainty in Climate Model Projections of Arctic Sea Ice Decline: An Evaluation Relevant to Polar Bears

By Eric DeWeaver

Abstract

This report describes uncertainties in climate model simulations of Arctic sea ice decline, and proposes a selection criterion for models to be used in projecting polar bear (*Ursus maritimus*) habitat loss. Uncertainties in model construction are discussed first, both for climate models in general and for their sea ice component models. A key point in the discussion is that the inherent climate sensitivity of sea ice leads inevitably to uncertainty in simulations of sea ice decline. The ability of climate models to simulate gross properties of Arctic ice cover, including the annual mean, seasonal cycle, and recent trends, is then assessed, followed by a review of model projections of 21st Century decline. The proposed selection criterion selects models with less than 20% error in their simulations of present-day September sea ice extent, where extent is defined as the area of the Arctic with at least 50% ice cover. Of the 10 models satisfying this criterion, all lose at least 30% of their September ice extent, and 4 lose over 80% of their September ice by the middle of the 21st Century (years 2045 to 2055). By the end of the 21st Century (years 2090 to 2099), seven of the models are essentially ice free in September.

Introduction

The U.S. Fish and Wildlife Service (USFWS) proposed listing the polar bear as a threatened species under the Endangered Species Act in January 2007. To help inform their final decision, they requested that the U.S. Geological Survey (USGS) conduct additional analyses about polar bear populations and their sea ice habitats. Between February and August 2007, USGS and collaborators developed nine reports targeting specific questions considered especially informative to the final decision. This is one of the nine reports. This report addresses climate model projections of Arctic sea ice decline, focusing on factors contributing to uncertainty in those projections.

This report has two goals. First, I describe the kinds of uncertainty inherent in climate models, particularly those uncertainties that directly affect the reliability of their projection of future Arctic sea ice conditions. The purpose of this description is to provide background helpful to polar bear scientists and managers, because an understanding of the future for polar bears necessarily requires an understanding of projections of sea ice. Second, I propose a criterion for selecting a subset of the available climate models for use in projections of future polar bear habitat. A simple and justifiable selection criterion was needed for the other analyses conducted as a part of this total effort—specifically for the analysis of predicting future distribution of polar bear habitat in the pelagic Arctic (Durner et al. 2007) and for projecting future size of the Southern Beaufort Sea polar bear population (Hunter et al. 2007).

Arctic sea ice has been in decline for decades (e.g., Richter-Menge, 2006; Meehl et al. 2007; Stroeve et al. 2007), with successive record-breaking low values in 2002, 2005, and 2007 (National Snow and Ice Data Center, *http://www.nsidc.org*), and climate models project greater sea ice losses for the remainder of the century (Section 3 below). Spatial and temporal reductions in sea ice cover and associated changes in sea ice character have been shown to impact negatively polar bears in some portions of their range (Stirling et al.

1999; Obbard et al. 2006; Regehr et al. 2006; Stirling and Parkinson 2006; Fischbach et al. 2007). Because they depend upon sea ice for nearly all aspects of their life history (Amstrup 2003), continuing sea ice declines projected by climate models could reduce the welfare of polar bears across much of their range. To appreciate what the future holds for polar bears, it is necessary to understand how changes in sea ice can affect polar bear distribution and numbers. It is also necessary to understand the uncertainties which affect the reliability of sea ice projections from climate models.

Climate models are computer programs developed at government and academic laboratories around the world to create detailed simulations of the Earth's global climate system. In the U.S., modeling centers include the National Center for Atmospheric Research (NCAR, in Boulder, CO), the Geophysical Fluid Dynamics Laboratory (GFDL, in Princeton, NJ), and the Goddard Institute for Space Studies (GISS, in New York, NY). A list of the 23 modeling centers that contributed simulations to the Intergovernmental Panel on Climate Change (IPCC) Fourth Assessment Report (AR4), with brief descriptions of the climate models, is provided in Table 8.1 of Randall et al. (2007). While these models have been used extensively in making projections of future climate, their primary purpose is the scientific investigation of climate, climate variability (e.g. the El Niño phenomenon), and the evolution of climate in response to orbital cycles, volcanoes, solar fluctuations, greenhouse gas concentrations, and other factors.

The fundamental physical laws encoded in climate models are well established, and the models are broadly successful in simulating present-day climate and recent climate change (Randall et al. 2007). For Arctic sea ice, model simulations unanimously predict declines in areal coverage and thickness due to increased greenhouse gas concentrations. They also agree that greenhouse gas-induced warming will be largest in the high northern latitudes and that the loss of sea ice will be much larger in summer than in winter (Meehl et al. 2007, Section 10.3.3).

Despite this qualitative agreement, climate model projections of Arctic sea ice decline span a considerable range, and guidance from models often is expressed in terms of the typical behavior of an ensemble of simulations. For example, Arzel et al. (2006) and Flato et al. (2004) show plots of the percentage of model simulations that have sea ice at each gridpoint over the Arctic Ocean in a 20th Century climatology. Arzel et al. (2006) also give the September Arctic sea ice loss averaged over all simulations (61% between the ends of the 20th and 21st centuries) and the fraction of models in which September was ice free in the later period (50%). Similarly, Holland et al. (2006b) report that episodes of abrupt sea ice loss occur in over 50% of the future climate simulations examined in their study.

While most aspects of climate simulations have some degree of uncertainty, uncertainty in projections of Arctic climate change is relatively high (Randall et al. 2007, Section 8.3). To some extent, the high level of uncertainty is a simple consequence of the smaller spatial scale of the Arctic, since climate simulations are reckoned to be more reliable at continental and larger scales (Meehl et al. 2007, Section 105.4.3; Randall et al. 2007). The uncertainty is also a consequence of the complex processes that control the ice, and the difficulty of representing these processes in climate models. The same processes which make Arctic sea ice highly sensitive to climate change, the ice-albedo feedback in particular, also make sea ice simulations sensitive to any uncertainties in model physics (e.g., the representation of Arctic clouds).

In assessing Arctic sea ice simulations, two prominent sources of uncertainty should be considered. First, uncertainties in the construction of climate models should be identified. While all models are constructed using the same physical laws, different approximations and simplifications are used in different models, and these differences lead to different sea ice simulation outcomes. Second, the degree of uncertainty due to unpredictable

natural variability of the climate system should be examined. The atmosphere, ocean, and sea ice comprise a nonlinear chaotic system with a high level of natural variability unrelated to external climate forcing. Even if climate models contained a perfect representation of all climate system physics and dynamics, inherent unpredictability would prevent us from issuing detailed forecasts of climate change beyond about a decade. Unpredictability is especially important in model-observation comparisons, since the large natural variability of Arctic sea ice must be distinguished from the effects of external climate forcing. The uncertainty in model simulations should be assessed through detailed model-to-model and model-to-observation comparisons of sea ice properties like thickness and coverage. In principle, inter-model sea ice variations are attributable to differences in model construction, but attempts to relate simulation differences to specific model differences generally have not been successful (e.g., Flato et al. 2004).

A practical consequence of uncertainty in climate model simulations of sea ice is that an ensemble of simulations should be considered in deciding the likely fate of Arctic sea ice. Some model-to-model variation in future sea ice behaviors is expected even among high-quality simulations, but part of the inter-model spread may be a consequence of poor simulation quality. Thus, it is desirable to define a selection criterion for membership in the ensemble, so that only those models that demonstrate sufficient credibility in present-day sea ice simulation are included. Fidelity in present-day sea ice simulation is an important consideration, since biases in present-day simulation have been linked to model behavior in projections of future sea ice decline (e.g., Holland and Bitz 2003).

This document discusses the forms of uncertainty listed above and the selection of models for consideration in assessing likely habitat loss for polar bears. The results of studies examining the models' ability to simulate the gross features of Arctic sea ice are reviewed, and the criterion for selecting models deemed most reliable for predicting future sea ice status as it relates to polar bears is described. I begin with a general discussion of uncertainties in model construction in Section 1, followed by a discussion of model performance in Section 2, which also discusses verification of models against available observations. Future projections of sea ice and their uncertainty are discussed in Section 3, and the selection of models for inclusion in the ensemble used by USGS is discussed in Section 4. Conclusions follow in Section 5.

I make the assumption that readers of this report have some familiarity with the efforts of the IPCC and its periodic assessment reports describing the growing worldwide knowledge of climate change due to increased greenhouse gases. The results of the most recent assessment report (AR4) are summarized in its Summary for Policy Makers (Solomon et al. 2007), and a history of the IPCC effort is given in Somerville et al. (2007).

1. Climate and Sea Ice Model Formulation

Like the real-world climate system, climate models and the sea ice models contained in them are quite complex, as is any discussion of their uncertainties. The discussion presented here begins with a general description of climate models and some of the approximations required in their construction. This general discussion is followed by consideration of two issues which contribute to uncertainty in climate models: 1) the need to "parameterize" processes which cannot be explicitly represented in the model (Section 1.1.1), and 2) the drift of the model climate towards an equilibrium state which is somewhat different from the observed climate (Section 1.1.2). Next, the sea ice component model within the climate model is described, both in terms of the thermodynamics of sea ice growth and melt (Section 1.2.1) and the dynamics of sea ice motion (Section 1.2.2). An additional section (1.2.3) discusses some of the uncertainties in the simulation of the

atmosphere and ocean that cause uncertainty in the simulation of sea ice. Finally, some improvements in the present generation of climate models over their recent predecessors are mentioned in Section 1.3. The goal of this section is to give the reader a general sense of what climate models are and why uncertainties inevitably are built into them.

1.1 Climate models

Climate models use the laws of physics (e.g., conservation of mass, momentum, and energy) to simulate the main components of the climate system: the atmosphere, ocean, land surface, and sea ice. The term atmosphere-ocean general circulation model (AOGCM) is also used for these models, to distinguish them from energy balance models and "Earth system models of intermediate complexity," which simulate the gross aspects of climate in simpler ways. Like the global models used for weather forecasting, the atmospheric component model tracks the time evolution of the state of the atmosphere, and climate simulations contain realistic representations of atmospheric features such as midlatitude weather systems, jet streams, and monsoons. As in global weather forecast models, the time step used for the atmospheric component model is generally less than one hour. Climate models go beyond weather forecast models in that they also represent the time evolution of the oceans, sea ice, and land surface, and the interaction of these components with each other through exchanges of energy, momentum, and moisture. The climates simulated by these models have been verified against observations in several model intercomparison programs (e.g., Achuta Rao et al. 2004; Randall et al. 2007) and been found to be generally realistic. Additional confidence in model simulations comes from experiments with a hierarchy of simpler models, in which the dominant processes represented by climate models (e.g., heat and momentum transport by midlatitude weather systems) can be isolated and studied.

Figure 1 illustrates some of the physical processes that determine the thickness and areal coverage of Arctic sea ice. The formation and growth of sea ice requires a loss of energy from the sea surface occurring at or below the freezing temperature. Thus, the loss of heat due to longwave (or infrared) radiation from the surface (labeled “L” in the diagram) contributes to ice formation and growth, as do surface heat losses due to heat conduction, evaporation, and sublimation (labeled “F” for heat flux). Sunlight absorbed at the surface promotes melt and inhibits ice growth, and the high albedo (or reflectivity) of ice and snow reduces the amount of solar energy absorbed at the surface. Clouds play a dual role since they shade the surface and reduce solar heating, but they also provide energy to the surface in the form of downwelling, longwave radiation. The polar cap receives a substantial amount of atmospheric energy from subpolar latitudes, both in the form of thermal energy (the “T” in the lateral arrow) and water vapor (“q”), which releases heat as it condenses to form precipitation (“P”). Much of the atmospheric energy transfer occurs through the movement of warm and cold air masses in weather systems. Ocean currents also bring heat into the Arctic and the export of ice from the Arctic to the North Atlantic constitutes an effective heat source for the Arctic. Realistic representation of these and other processes is essential for successful simulation of the climate and sea ice of the Arctic.

Despite their considerable recent evolution (Kattsov et al. 2005; Somerville et al. 2007) and their general success in simulating present-day conditions, climate models have significant limitations. A variety of simplifications are necessary for the relevant physical laws to be implemented as computer programs. Thus, the laws of physics operating in a climate model must be an approximate form of the true governing laws and models can be distinguished from one another according to how these approximations have been made.

The most obvious form of approximation is the discretization of the equations for the time evolution of the component models. The state of the climate system is represented in three

dimensions by the values of appropriate variables (e.g., temperatures, winds, currents) on a global mesh of gridpoints at the Earth's surface and at several vertical levels in the atmosphere and ocean. The grid spacing (i.e., model resolution) is limited by the availability of computing resources, and models differ in total resolution, the amount of resolution given to each component model, and the manner in which the governing equations are expressed at the gridpoints. For example, the grid spacing used in the atmospheric component model of the NCAR Community Climate System Model, version 3 (CCSM3) is roughly 100 km, with 26 vertical levels, while the grid spacing for the ocean (40 levels) and sea ice models ranges from 25 to 80 km, depending on latitude (Collins et al. 2006). This resolution is high compared to most simulations for the AR4.

1.1.1 Subgrid-scale Parameterization and Model Tuning

Resolution of current models is sufficient to capture all the large-scale features of atmospheric circulation, including typical mid- and high-latitude cyclones. However, many of the processes of interest in the climate system occur on spatial scales too small to be resolved. Thunderstorms, for example, would fall entirely between the gridpoints of the atmospheric component model. Phenomena which cannot be explicitly resolved are "parameterized," or represented implicitly in terms of resolved variables. The parameterization of subgrid-scale phenomena is perhaps the primary source of uncertainty in model construction. The rules relating unresolved processes to the resolved state of the system, in general, cannot be derived from fundamental laws of physics alone. Rather, modelers use a number of different parameterizations to represent or approximate the same phenomenon. For example, the fractional coverage of stratiform clouds is often parameterized as a function of relative humidity (e.g., Boville et al. 2006). This relationship, though physically reasonable, only crudely represents the many ways in which real-world cloudiness depends on the resolved-scale variables represented at the climate model gridpoints. One way in which this parameterization simplifies the dependence is by ignoring the role of aerosols in cloud formation (e.g., Gorodetskaya et al. 2007). Thus, parameterization schemes represent a balance between the need for simplicity and computational efficiency, and the desire to account for all relevant processes. While it would be desirable to add aerosol effects to the cloud fraction parameterization, doing so would require specification of aerosol properties and amounts, which would further require simulation or parameterization of aerosol emissions, transport, and chemical reactions.

Formulas used in parameterization schemes usually involve several parameters whose values cannot be determined from observations or theory, and which thus can be adjusted to improve overall model performance. One example is the minimum relative humidity threshold used in the above-mentioned cloud fraction parameterization. In reality, clouds form when the local relative humidity reaches or slightly exceeds 100%. Such saturation occurs on the cloud scale but not the large scale represented by an atmospheric model gridpoint. Lowering the threshold is physically justifiable, but there is no formally correct value, and the threshold is simply adjusted, within reason, to give good performance on a global basis.

The process of adjusting these parameters is often referred to as "tuning." For example, Hack et al. (2006) note that some tuning is necessary in order to achieve a balanced energy budget for the simulation of present-day climate. They also note that this tuning is done through trial and error, and that the tuning must be revised whenever model resolution is increased. Randall et al. (2007) suggest that tuning is acceptable, provided that the values of the tuned parameters do not exceed reasonable bounds and that the number of tunable parameters is small compared to the number of observational constraints used in model evaluation. The second criterion, which is believed to be satisfied by most climate models (Randall et al.

2007), prevents modelers from exaggerating the quality of their models by evaluating them against the same observations used to tune them. Tuning parameters do not vary in time or space, so evaluating models based on their performance in a number of geographical regions as well as their representation of interannual variability (e.g. variability associated with El Niño events or the North Atlantic Oscillation) guards against such over-tuning. Since tuning introduces arbitrary choices into climate models, and even into the same model when used at different resolutions, it constitutes a large source of uncertainty in climate model construction.

The simulation produced by a climate model represents the effects of all parameterizations used in it, and it is possible that a successful simulation can be achieved because a bias in one parameterization is counteracted by an opposing bias in another. For example, the thickness of sea ice is sensitive to the amount of solar radiation it absorbs during the melt season. Thus a cloud parameterization which allows too much sunlight to reach the surface can be compensated by an albedo parameterization in the sea ice component model which reflects too much sunlight back to space, thereby yielding appropriate solar absorption. This sort of compensation is an issue for climate change studies, since different combinations of albedo and cloudiness may produce the same present-day sea ice thickness but differing estimates of future climate change, since the climate change depends on the strength of the sea ice-albedo feedback (section 1.2.1) which will be stronger with fewer clouds. The presence of such compensations is difficult, though not impossible, to detect.

1.1.2 Spin-up, Climate Drift, and Flux Adjustment

Each component model of a climate model is developed in "stand-alone" mode, with observational data substituted for the inputs it requires from the other component models. The atmospheric model in stand-alone mode uses observed sea surface temperatures and sea ice cover rather than obtaining these inputs from the sea ice and ocean component models. Since the atmospheric component model is developed to give the best possible simulation with observed sea surface temperatures and sea ice, the atmospheric simulation will necessarily be less than optimal when the atmospheric model takes its inputs from the ocean and sea ice models instead. The ocean and sea ice models, which are designed to give best performance with real-world atmospheric inputs, will also produce less realistic simulations when their inputs come from the atmospheric model. When coupled to form a climate model, the "drift" of the ocean and sea ice models away from their observationally-driven simulations will produce a further drift of the atmospheric model away from its stand-alone simulation. Thus the climate simulation produced by coupling the component models together can be significantly different from the observed climate even if the component models perform reasonably well in stand-alone mode. Furthermore, the drift of the simulated climate can proceed over a long "spin-up" period before a steady-state climate simulation is achieved.

Climate drift can be minimized through the process of "flux adjustment", in which the outputs of the component models are modified before being used as inputs to the other component models. For example, the fluxes of heat and moisture from the ocean to the atmosphere could be corrected before applying them to the atmospheric model in order to produce a more realistic atmospheric simulation (e.g. Meehl 1992; Kattsov et al. 2005). Flux adjustments represent a trade-off in modeling: the adjustments are not desirable, since they do not represent real physical processes, yet they may be necessary to prevent the climate model from drifting to an unrealistic climate. As discussed in section 1.3, improvements in climate modeling have greatly reduced the use of flux adjustments. Flux adjustments used in IPCC models are listed in Table 8.1 of Randall et al. (2007).

The spin-up period required for a climate

model to achieve a steady-state equilibrium climate can be quite long, even several hundred years, due to the slow overturning motion of the deep oceans. Simulations of climate change must begin with a fully spun-up climate to avoid confusing climate drift with climate change due to increases in greenhouse gas concentrations. Thus, it is not possible to initialize a global warming simulation with a specified present-day climate state. In this respect climate models differ from weather forecast models, in which the forecast model is initialized with the best possible representation of the current atmospheric state and the quality of the forecast depends on the quality of the initialization.

1.2 Sea Ice Component Models

The sea ice component model typically simulates fractional ice coverage (percent ice-covered area per unit surface area of ocean, or concentration), mean ice thickness, ice motion, temperature and many other ice properties such as albedo (surface reflectivity), snow accumulation, and energy fluxes into and out of the ice. Sea ice model calculations can be categorized as thermodynamic or dynamic, with the former determining the rate of growth and melt of the ice through heat gain and loss, and the latter determining the resolved-scale movement of the ice and the subgrid-scale redistribution of ice by differential movement. On a fundamental level, the thermodynamics of ice growth and melt are determined by conventional heat conduction and the latent heat of freezing and melting while ice motion is governed by a momentum conservation equation. However, the application of these physical laws to produce a practical sea ice component model requires a variety of simplifications and parameterizations which add uncertainty to climate model construction.

1.2.1 Thermodynamics of Growth and Melt in Sea Ice Models

Sea ice forms when the ocean surface temperature falls to approximately -1.8°C and small ice particles agglomerate to create a slush of ice crystals called frazil ice. As the ice grows it expels salt in a process called brine rejection, which makes the salinity of the ice dependent on its age. Salt content is important for ice due to its effect on thermal conductivity and also because the melting of ice is affected by small "brine pockets" of unfrozen salty water trapped in the ice. The salinity of ice is determined by microphysical processes which must, of course, be parameterized. A further issue for ice growth is the amount of snow on top of the ice, since snow is a better insulator than ice and thus reduces ice growth by slowing the rate at which heat is lost through the ice by the underlying ocean. The accumulation, melting, flooding, sublimation, and refreezing of the snow are accounted for in a variety of ways in sea ice models.

The amount of ice that melts in summer is sensitive to the snow and ice albedo, which can be parameterized as a function of temperature, ice thickness, amount of snow cover, snow age, and snow melt. Real-world sea ice albedo is correspondingly complex, since snow albedo is higher than ice albedo, and much of the sunlight that contributes to ice melt is absorbed not by ice and snow but by melt ponds on the ice which have lower albedo. The challenge of parameterizing surface albedo is apparent in Figure 2, which gives an aerial view of the sea ice near the end of the melt season during the 1998 Surface Heat Budget of the Arctic (SHEBA; Uttal et al. 2002) field experiment. Snow-covered sea ice presents a highly reflective surface to sunlight, while melt ponds on the surface have a light blue appearance and absorb much more of the sunlight which falls on them, and dark patches of open ocean absorb up to 90% of the sunlight they receive. Albedo values calculated at a model gridpoint must incorporate the effects of all these surface types averaged over the grid spacing of the model. In

addition, the model must account for the portion of sunlight which goes through the surface of the ice, warming and melting the interior without changing ice thickness or passing through the ice to warm the ocean below.

The proper representation of surface albedo is particularly important in light of the sea ice-albedo feedback, a positive feedback in which the melting of sea ice or snow on sea ice reduces surface albedo, allowing more of the incident sunlight to be absorbed at the surface. When more sunlight is absorbed rather than reflected, the additional gain of heat energy leads to more melting, which further lowers albedo, allowing even more absorption of sunlight, more melting, and so on. Sea ice-albedo feedback is perhaps the primary reason for the enhanced sensitivity of Arctic climate to greenhouse gas increases (e.g. Manabe and Stouffer 1980), and the increased absorption of sunlight in the Arctic may significantly increase the warming of the whole globe due to CO_2 increase (Rind et al. 1995). Model-to-observation comparisons of the sea ice-albedo feedback are not available, but a study of the snow-albedo feedback over land (i.e., snow melt exposes a darker surface, promoting solar absorption and further melting) showed that models tend to underestimate the feedback (Hall and Qu 2006).

The growth of sea ice in winter depends on the rate at which heat is lost from the ocean below the ice to the atmosphere above -- a rate which is strongly dependent on the thickness of ice (e.g., Bitz and Roe 2004). Even in regions of thick perennial ice there is always some open water in the form of leads (linear openings or cracks in the ice) and polynyas (larger areas of open water). These are regions of intense heat loss from the ocean and subsequent growth of new ice, and their effect must be included in sea ice models despite their subgrid spatial scale. In addition to open water fraction, a resolved-scale region in the Arctic ice pack will also contain ice of a variety of thicknesses, and this subgrid-scale variability is important for ice growth. Bitz et al. (2001) cite studies which show that ice growth rates in the central Arctic roughly double when averaged over a realistic distribution of thicknesses compared to the growth rate obtained assuming only the mean thickness for the distribution. Subgrid-scale thickness distributions are now included in many but not all sea ice component models.

The sensitivity of sea ice to global climate change can be appreciated by considering that a heating rate of 1 Wm^{-2} (1 watt per square meter) applied to the ice for a year would melt about 10 cm of sea ice (for comparison, the melt season-averaged solar heating rate for sea ice observed during the SHEBA experiment was about 60 Wm^{-2}; M. Holland, personal communication). A typical estimate of increased surface heating due to CO_2 doubling is about
4 Wm^{-2} which, in the absence of any other effects, would melt through 3 m of ice (close to the mean thickness for Arctic sea ice) in less than a decade. In winter (nighttime in the Arctic), areas of ice-free ocean surface are warm compared to the overlying atmosphere, so the ice-free regions cool quickly until new ice forms and provides insulation from the cold atmosphere. This heat loss from ice free surface waters accounts for global warming simulations in which the Arctic sea ice melts away each year by September, yet a relatively expansive ice cover still develops over the winter months.

Studies which model the growth and melt of a single column of sea ice often find very large sea ice thickness sensitivity to relatively small variations in snow cover and heat fluxes from the atmosphere and ocean (Maykut and Untersteiner 1971; Semtner 1976; Ebert and Curry 1993). This sensitivity is presumably inherent in the form of the heat conduction equation that determines the growth of the ice rather than a consequence of parameterization choices. But Randall et al. (1997) note that models which include ice motion tend to have much smaller sensitivities. DeWeaver et al. (2007) analyze a climate model experiment in which sea ice albedo is deliberately increased and the effect of the increase on sea ice thickness is examined. The albedo increase leads to a thickness increase which is partially

offset by the movement of the thicker sea ice out of the Arctic. Inherent sensitivity is an important issue, because significant errors in solar and infrared radiation are expected due to errors in Arctic cloud simulation (e.g., Beesley and Moritz 1999; Vavrus 2004). These errors will produce errors in ice thickness and extent to varying degrees depending on the inherent sensitivity of the sea ice.

1.2.2 Dynamics of Resolved and Subgrid-Scale Motion in Sea Ice Models

Sea ice moves in response to top and bottom stresses exerted by the atmosphere (surface wind stress) and ocean, the tilt of the ocean surface, the Coriolis force, and internal stress within the ice cover (e.g., Hibler and Flato 1992; Parkinson and Washington 2005). On the resolved scale, motion is a key determinant of regions of thick and thin ice within the Arctic, and accounts for much of the error in simulations of the Arctic thickness pattern (Bitz et al. 2002; Randall et al. 2007). Motion is also important for the total volume of ice in the Arctic; Rothrock and Zhang (2005) find that about 12% of the Arctic ice volume is lost to export each year. Ice motion also plays a crucial role on the subgrid-scale, as differential ice motion causes the opening of leads, the formation of ridges, and the rafting of ice floes on top of each other. The thickness distribution is determined by the competing effects of thermodynamics processes which tend to reduce the variability of thickness and dynamic effects which produce adjacent patches of open water and very thick ice (Thorndike et al. 1975).

Simulation of resolved-scale ice motion requires specification of the effective net force due to internal stresses caused by collisions, breakups and pile-ups within the pack. The most important result of internal ice stress for ice motion calculations is to resist the build-up of ice that would otherwise occur due to wind-induced convergence of ice (Hibler and Flato 1992). The net force consists of a pressure component which depends on the thickness and fractional coverage of the ice, and compressive and shearing stresses dependent on the differential motion of the ice (Hibler 1979; Hibler et al. 1992; Hunke and Dukowicz 1997; Parkinson and Washington 2005). The most sophisticated representation of the ice stress in the IPCC simulations is the viscous-plastic rheology introduced by Hibler (1979) and its modification by Hunke and Dukowicz (1997), who introduced a more computationally tractable elastic-viscous-plastic (EVP) rheology. A simpler representation of ice stress is the cavitating fluid rheology (e.g., Hibler et al. 1992), which includes only the pressure (neglecting the shear strength). On the subgrid-scale, the effect of ice motion on the thickness distribution is often represented by a mechanical redistribution function, which represents the creation of thick ice from thinner ice through ridging and rafting (Thorndike et al. 1975).

Some appreciation of the issues involved in modeling ice motion can be gained from Figure 3, which shows the movement of ice through the Bering Strait in early May (the beginning of the melt season). The resolved-scale motion consists of an export of ice from the Arctic driven by surface winds which, to the extent that the wind pushes ice floes together, will be resisted by an internal pressure force which must be parameterized. On the subgrid-scale, differential ice motions are responsible for the leads seen in the upper left corner of the figure, and the lead fraction must be parameterized due to the importance of the strong heat fluxes that occur in the leads.

Representations of ice stress and mechanical redistribution cannot be formally derived from the basic material properties of sea ice, but they are constrained by “common sense” physical principles. For example, mechanical redistribution is carried out in ways that conserve ice mass, and ice stress is usually set to zero under diverging conditions, since ice floes do not resist being blown away from each other. The performance of state-of-the-art sea ice models has been extensively tested in offline calculations, in which simulated sea ice melts, grows and moves under the influence of

atmospheric conditions specified from available observations (an ocean model is also used in these simulations). Parkinson and Washington (2005) summarize several studies of this sort, including calculations by Zhang et al. (1999) in which simulated sea ice motion follows closely the trajectories of the drifting buoys of the International Arctic Buoy Program (IABP, see Rigor et al. 2002), and fractional ice coverage is in good agreement with satellite observations.

1.2.3 Atmospheric and Oceanic Simulation Uncertainties of Consequence to Sea Ice

Sea ice grows and melts according to its loss or gain of thermal energy, so the ice is necessarily sensitive to simulation deficiencies in other component models which affect these gains and losses. In the atmospheric component model, factors which strongly influence the sea ice simulation include the temperature profile of the atmospheric boundary layer (the lower portion of the atmosphere which is directly influenced by the surface, typically the lowest 1 km or less over the Arctic Ocean), the representation of clouds, and vertical heat fluxes within the boundary layer. Kattsov et al. (2005) point out that vertical resolution of the atmospheric component model may be too coarse to capture the strong but shallow temperature inversions which form above sea ice during the Arctic winter.

Studies including Vavrus (2004), Beesley and Moritz (1999), and Walsh et al. (2002) note that models have difficulty in simulating cloud fraction (the fraction of the sky covered by clouds) over the Arctic, and the mean annual cycle of cloudiness averaged over the Arctic ocean is generally not captured in either stand-alone atmospheric models or climate models. Randall et al. (1997) note the presence in the Arctic of multiple layers of clouds in the summertime boundary layer, which presents difficulties for models both because of limited vertical resolution and the lack of understanding of the physical mechanisms involved. They also note difficulties in representing vertical fluxes of heat, momentum, and moisture in the wintertime boundary layer, which is generally very stable but broken up sporadically by plumes of warmer moist air rising from areas of open water (leads), which form between ice floes. "Arctic haze" (industrial aerosol pollution which enters the Arctic primarily from Eurasia, e.g., Shaw 1995) and clear-sky ice crystal precipitation pose further challenges to the parameterization of Arctic clouds. Cloud errors are particularly significant for sea ice simulation because clouds regulate the amount of sunlight at the surface during summer and provide a source of downwelling infrared radiation during the winter. Thus, they substantially moderate both the growth and melting of the ice.

Sea ice is also sensitive to the simulation of the ocean component model, since ice can be melted by ocean heat flux. Maykut and Untersteiner (1971) found that an increase of about 5 Wm^{-2} in ocean heat flux convergence (OHFC) was sufficient to melt all the ice in their model of a column of sea ice at a single point (they estimate that present-day OHFC is about 2 Wm^{-2}). Tremblay et al. (2007) find that an increase of 17 Wm^{-2} in OHFC removes most of the ice in their model of sea ice cover over the whole Arctic. Ocean heat flux into the Arctic occurs as warmer Atlantic water (AW) enters the basin. This water is denser than the surface water and thus sinks to form a layer between depths of 100 and 800 m (Quadfasel et al. 1991) with a core temperature significantly above freezing. Sea ice is buffered from the heat carried by the AW because Arctic surface waters are relatively fresh and thus less dense than the AW, which is separated from the upper ocean by the sharp salinity gradient of the Cold Halocline Layer (CHL). Tremblay et al. (2007) show that models have difficulty simulating the CHL and may thus allow too much heat from the AW to reach the ice. Ocean biases have several sources, including insufficient vertical resolution in the ocean component model, wind errors in the North Atlantic driving too much or too little AW into the Arctic, and insufficient information about precipitation over subarctic landmasses, since the freshness of the Arctic

Ocean is partly due to river discharge.

In addition to the thermodynamic influence of the atmosphere and ocean on the sea ice simulation, sea ice dynamics render the sea ice sensitive to the effects of surface wind errors in the atmospheric component model. Bitz et al. (2002) demonstrated that surface wind errors in many atmospheric models are sufficient to cause large errors in the pattern of sea ice thickness across the Arctic, since errors in surface wind direction pile up the ice on the Siberian coast, in opposition to the observed maximum on the Canadian side. The wind errors are associated with a tendency for Arctic sea level pressure to be too high. In the northern hemisphere, winds circulate clockwise around high pressure centers, so an erroneous polar high is accompanied by an erroneous east-to-west circulation around the pole (see also Walsh et al. 2002).

1.3 Climate and sea ice model development

Climate models are continually under development, and the models used in the IPCC AR4 are substantially improved over those available in the IPCC Third Assessment Report (TAR, IPCC 2001) and even the more recent Arctic Climate Impacts Assessment (Kattsov et al. 2005). One driver of model improvement is increases in computer resources, which have enabled substantial increases in model resolution. The atmospheric component model used in the NCAR CCSM3 simulations has a horizontal resolution four times higher than the earlier version used in the TAR and with 26 vertical levels rather than the earlier 18. A second significant improvement is reduced reliance on flux adjustments (section 1.1.2): Six of the 23 climate models used in AR4 had some form of flux correction, compared to 17 out of 31 in the TAR. Additional improvements in parameterization of climate processes can be found in Randall et al. (2007), who also discuss recent increases in the amount of scrutiny to which model simulations have been subjected, particularly in model intercomparison projects such as the Coupled Model Intercomparison Project (CMIP; Achuta Rao et al. 2004; Meehl et al. 2005).

Sea ice component models have improved substantially in recent years. Flato et al. (2004) summarize the sea ice component models for climate models participating in the second CMIP Project (CMIP2; Achuta Rao et al. 2004; Meehl et al. 2005). Of 16 models, 9 had motionless sea ice and 4 used "free drift", in which the ice drifts with the ocean surface current (a cutoff thickness is usually used to prevent excessive ice build-up). Only three used a full representation of internal ice stress (Holland and Bitz 2003 provide a similar listing). Similarly, only 2 of 31 climate models used in the TAR had sea ice motion. In comparison, two models used in the AR4 had motionless ice, two have free drift (Randall et al. 2007) and the remaining 19 use some form of internal ice stress. A more detailed description is provided for a subset of 15 models by Zhang and Walsh (2006), who report that 9 models use viscous-plastic or EVP rheology, 4 use the simpler cavitating fluid rheology and 2 others use free drift. The use of thickness categories is somewhat limited in AR4, with only 5 models incorporating a thickness distribution, and only two with time evolving thickness distributions (HadGEM1 and CCSM3, both noted for their realistic present-day simulations and dramatic sea ice loss in future simulations). However, all AR4 models contain a parameterization for the opening and closing of leads to ensure that some open water is present even in a thick ice pack.

Randall et al. (2007) note that recent advances in sea ice component models have not resulted in dramatic improvements in sea ice simulations. They note that the continued presence of significant sea ice errors can be attributed to errors in the atmospheric and oceanic component models which provide inputs to the sea ice. This verdict is consistent with the experience of Zhang et al. (1999), who showed that sea ice models are capable of producing high-quality simulations when forced with realistic surface winds and temperature.

Bitz et al. (2002) and DeWeaver and Bitz (2006) use offline sea ice thickness calculations to show the effect of surface wind errors on simulated sea ice thickness.

In addition to specific model improvements, the availability of multi-model ensembles of climate simulations has motivated novel attempts to characterize and understand uncertainty in model simulations and projections. One such attempt is the climateprediction.net project (CPDN, Knutti et al. 2006), in which a coarse resolution climate model was distributed over the internet to users who conducted simulations on home computers. The idea of the project is to assess simulation uncertainty by conducting a very large number (over 2,500) of simplified climate simulations in which various tuning parameters are perturbed randomly over a range of reasonable values. One result of the project is a careful assessment of the uncertainty in future climate predictions owing to parameterization uncertainties. They find that the global warming for a doubling of CO_2 from its pre-industrial concentration (roughly the B1 scenario) is very unlikely (less than a 5% chance) to be below 1.5˚C, but the upper bound on possible warming is more difficult to assess. They challenge the range of 1.5 to 4.5˚C given in the TAR, saying that the upper bound for global temperature increase (less than a 5% chance of exceedance) is poorly constrained, and can vary between 5˚C and 6.5˚C depending on the assumptions of the analysis.

2. Verification of 20C3M Sea Ice Simulations

Uncertainties in sea ice model parameterizations and the inherent sensitivity of sea ice thermodynamics, combined with further uncertainties in atmosphere and ocean model construction, lead inevitably to errors in the simulation of Arctic sea ice. Several studies have examined the quality of climate model sea ice simulations in comparisons against available observations. Two categories of studies are possible: those which consider the mean state and seasonal cycle of the ice, and those which consider the variability of the ice, especially the decreasing Arctic sea ice trend in recent decades. Both types of studies are discussed in this section.

Comparisons for models participating in AR4 are often carried out using simulations from the archive of simulations of "20th century climate in coupled models" (20C3M, Meehl et al. 2005). The radiative forcing used in these simulations is not uniform across the ensembles, as some modeling centers used more radiative inputs than others, e.g. sulfate aerosols, volcanic emissions, black carbon and solar variability (all include sulfate aerosols and increasing levels of carbon dioxide). A listing of models and their 20C3M radiative inputs is provided in Table 10.1 of Meehl et al. (2007). 20th century simulation comparisons are also available for models participating in the earlier CMIP and CMIP2 projects. Typically, present-day simulations are started from a pre-industrial simulation in which the climate model is run for a long period of time (360 years, in the case of CCSM3) using greenhouse gas levels appropriate for the pre-industrial era.

2.1 Mean state and annual cycle

The discussion below reviews several studies which compare observed and simulated thickness and areal coverage of Arctic sea ice. The quality of some atmospheric quantities of importance to the ice simulation (e.g. clouds) is also assessed. A common finding in these assessments is that mean quantities averaged over an ensemble of model simulations are often in better agreement with observations than the simulation from any given model.

2.1.1 Concentration and areal coverage

The total area covered by sea ice is the simplest and most integrative point of comparison between models and observations. Northern Hemisphere sea ice extent is usually defined as the area of the Northern Hemisphere

oceans with at least 15% ice coverage. It is closely related to sea ice area, which is the spatial integral of sea ice concentration over the Northern Hemisphere. “Area” is a more precise measure, since it takes lead fraction into account, but “extent” is more reliably observed (Zhang and Walsh 2006). Sea ice concentration data are available from all-weather satellite observations starting in 1978 (e.g., Cavalieri et al. 1999), supplemented with earlier ship and aircraft measurements (Raynor et al. 2003).

Zhang and Walsh (2006) considered 15 20C3M climate simulations and found that the models generally succeed in simulating an annual-mean sea ice area within 20% of observations. For the ensemble-averaged annual-mean area they obtained a value of 1.06×10^7 km^2, close to the observed value of 1.10×10^7 km^2 (their Table 2; one model with apparent spin-up problems is excluded). Relatively close agreement between the ensemble mean and available observations despite large ensemble spread is a recurrent theme in evaluations of model simulations.

A wider variation was found in the annual cycle of ice area, with the largest discrepancies occurring in August and September (September is usually the month of minimum coverage, while the maximum coverage is typically in March). Zhang and Walsh’s (2006) plots of the annual mean area and its seasonal cycle are reproduced here as Figure 4. The annual cycle in 20C3M ice extent simulations was also examined by Parkinson et al. (2006a, b), who find that all models capture the timing of the annual cycle. They also plot the ensemble-mean annual cycle, which is found to be close to the observed annual cycle, but with consistently higher values for extent (3% larger extent in December and 14% larger in September). Stroeve et al. (2007) found that 13 of the 21 models in the A1B 21st century climate change scenario ensemble (see section 3) had September sea ice fraction within 20% of observations.

The geographical distribution of sea ice in 20C3M simulations is shown by Parkinson et al. (2006a) and Arzel et al. (2006), and both studies find considerable differences among the simulations. Nevertheless, Arzel et al. (2006) find the median sea ice edge for the 20C3M ensemble in March and September (i.e., maximum and minimum coverage), and find that the median sea ice edge agrees reasonably well with observations (here the edge is the boundary between the region of the ocean with more than 15% ice coverage and the region with less). A similar level of agreement between the median sea ice edge of the ensemble and the observed sea ice edge was found by Flato et al. (2004) for the CMIP ensemble in both summer and winter.

2.1.2 Thickness

The mean and annual cycle of sea ice thickness in the 20C3M ensemble was examined by Gerdes and Koberle (2007), who again found large inter-model variations within the 20C3M ensemble. Since ice thickness is poorly observed, they compared the thickness simulations to six "hindcast" experiments from the Arctic Ocean Model Intercomparison Project (AOMIP, Proshutinsky et al. 2001), in which ocean-sea ice models simulated the period 1979 to 2001 using atmospheric forcing from observations (river runoff is also specified). As a gross measure of simulation quality they compared the total Arctic ice volume for 1985 to 2000 with the same quantity from the hindcasts. They find that of 18 models, 11 have ice volume within the range spanned by the six hindcasts, 15,000 and 30,000 cubic km. They also show the annual-mean, April, and September spatial distribution of thickness for some of the models. They note models which have an excessively pole-centered thickness pattern as well as models which have ice buildup along the wrong sections of Arctic coastline. They attribute these biases primarily to wind-induced anticyclonic ice drift. The single 20C3M simulation that uses motionless ice has a strongly pole-centered pattern. The best thickness patterns were found in CCSM3 and HadGEM1 (see list of acronyms for models and modeling centers).

2.1.3 Atmospheric quantities of relevance to sea ice

The presence of an anticyclonic surface wind pattern circulating around an erroneous Arctic high pressure center is a common problem in climate models (see section 1.2.3) and was documented for the 20C3M simulations by Chapman and Walsh (2007). They note that the high bias is less pronounced than in earlier generations of models. In addition to the detrimental effects of the anticyclonic winds on ice motion, high pressure is associated with a deficit of strong storms (low pressure systems) entering the Arctic from the North Atlantic, which is significant because storms push warmer ocean water into the Barents sea, reducing ice formation there. Thus the high pressure bias is associated with excessive sea ice in the Barents sea in most of the simulations. In CCSM3 the anticyclonic bias was largely alleviated by increasing the resolution of the atmospheric component model (DeWeaver and Bitz 2006). A second topic addressed by Chapman and Walsh (2007) is a tendency for Arctic surface air temperatures to be too cold, and they note that the overall performance of 20C3M simulated Arctic temperature is comparable to that of the models used in the TAR.

Large differences in simulations of fractional cloudiness in the Arctic are expected (see section 1.2.3), and Gorodetskaya et al. (2007) discuss the effect of cloud biases on sea ice simulations in three 20C3M simulations (from the CCSM3, HadCM3, and GISS-ER models). The models show pronounced differences in cloud fraction, although these differences are smallest during the melt season. There are also important differences in the radiative effects of the clouds due to differing amounts of liquid water and ice which cause the Arctic Ocean surface to gain 20% to 40% more energy during the melt period in the GISS-ER and HadCM3 models than in CCSM3.

A critical evaluation of 20C3M simulations is given by Eisenman et al. (2007), who claim that variations in downwelling longwave radiation are so large that they rule out meaningful simulations of sea ice thickness. They use simple arguments to estimate the spread in sea ice thickness that would be caused by differences in longwave flux (more longwave flux, thinner ice), and state that the inter-model range ought to be at least 10 m, while the actual 20C3M range is 1 to 4 m. They suggest that modelers have artificially prevented the larger range by making minute, nonphysical adjustments to sea ice albedo. This claim is not consistent with climate model experiments performed by Holland et al. (2006a) in which a 13% increase in ice albedo resulted in only a half meter increase in ice thickness, much less than the increase predicted by Eisenman et al.'s estimates. DeWeaver et al. (2007) noted several ways in which the more realistic physics of Holland et al.'s (2006a) climate model prevents the sort of fine-tuning of albedo claimed by Eisenman et al., including the effects of cloud cover and sea ice motion (also noted by Randall et al. 1997), neither of which is considered by Eisenman et al. (2007).

2.2 Trends in the observed record

The ability of climate models to project future sea ice decline should logically be judged by their ability to reproduce the downward trends of recent decades, shown in Figure 5. September Arctic sea ice extent declined by 7.8% per decade from 1953 to 2006 and 9.1% per decade for the period 1979 to 2006 (Stroeve et al. 2007), the years for which satellite data are available. September extent has had pronounced minima in every year since 2001, with successively lower record-breaking minimum extent values in 2002, 2005, and 2007 (*http://www.nsidc.org*). The 2005 minimum was a 21% reduction compared to the mean for 1979 to 2000 (Serreze et al. 2007). Sea ice extent reported by NSIDC on 28 August 2007 was 4.78 million km^2, well below the record absolute minimum extent of 5.32 million km^2 reported in 2005. This decline is consistent with evidence for Arctic warming from a variety of sources, such as surface air temperature

increases over land and ocean (e.g., Alley et al. 2003, Johannessen et al. 2004, Serreze and Francis 2005), thawing of Alaska permafrost (Osterkamp and Romanovsky 1999), and a transition in land cover from tundra to sub-Arctic shrub (Wang and Overland 2005).

Considering the magnitude of recent trends, one might expect them to provide a clear target for model evaluation and intercomparison. However, evaluation of 20th Century sea ice in model simulations is complicated by the large intrinsic variability of Arctic climate: this is the uncertainty due to unpredictability mentioned in the introduction. In the literature of natural Arctic climate variability two forms of variability feature prominently: 1) long-term wind fluctuations associated with the Arctic Oscillation (AO), and 2) variations in ocean heat flux due to incursions of Atlantic water (AW), together with reductions in the buffering effect of the cold halocline layer (CHL).

2.2.1 Influence of the Arctic Oscillation

The AO (Thompson and Wallace 2000; Thompson et al 2000) is also referred to as the Northern Hemisphere Annular Mode (Limpasuvan and Hartmann 2000), and closely related to the more regional North Atlantic Oscillation (NAO; e.g., Hurrell 1995). It can be approximately described as a meridional shift of atmospheric mass away from (in the high phase) or toward (in the low phase) the North Pole, accompanied by a poleward shift of the midlatitude westerly winds extending from sea level to the lower stratosphere in the high phase (an equatorward shift in the low phase). The AO is the most prominent mode of atmospheric variability in high northern latitudes, and it exhibited a pronounced trend toward higher values from 1970 to the mid-1990s (Thompson et al. 2000 show trend maps for 1968 to 1997).

Rigor et al. (2002) use IABP buoy data to document the effect of the AO on sea ice motion. They show that this shift to more counterclockwise surface winds over the Arctic causes thinning of the ice along the East Siberian and Laptev Seas (see the map of Arctic Ocean place names) by moving away multi-year ice, as well as increasing export of multi-year ice through Fram Strait (Fram Strait lies between the Northeast coast of Greenland and the island of Spitsbergen). The effect of the shift from anticyclonic to cyclonic wind circulation is shown in Figure 6 taken from Rigor et al. (2002). Rigor and Wallace (2004) go on to suggest that the recent reduction in September ice extent is a delayed reaction to the export of multi-year ice during the high-AO winters of 1989-1995. They estimate that the recovery of sea ice to its normal extent should take between 10 and 15 years. The notion of sea ice decline as a delayed reaction to the impulsive flushing of multi-year ice was challenged by Overland and Wang (2005), who note that no recovery is evident despite the return of the AO to a more neutral state. The winter values of the AO for 1960 to 2004 are shown in Figure 7, taken from Overland and Wang. Despite the mixed record of high and low AO years since 1995, the decline of sea ice extent has increased over the past 12 years, as noted above.

Recognizing the need to incorporate AO variability into considerations of recent sea ice decline, Lindsay and Zhang (2005) used an ocean-sea ice model to reconstruct the sea ice behavior of the satellite era and identify separate contributions from ice motion and thermodynamics. Similar experiments with similar results were also reported by Rothrock and Zhang (2005) and Koberle and Gerdes (2003). Lindsay and Zhang (2005) propose a three-part explanation of sea ice decline which incorporates both natural AO variability and an overall warming climate. In their scheme, a warming climate preconditions the ice for decline as warmer winters thin the ice, but the loss of ice extent is triggered by natural variability, in this case flushing by the AO. The loss continues after the flushing due to the sea-ice albedo feedback discussed in section 1.2.1 (more open water means more sunlight absorbed, which warms the surface and leads to additional sea ice melting). Their work suggests that the observed record is best interpreted as a combination of internal variability and external

forcing, and raises the possibility that the two factors may act in concert rather than as independent agents.

2.2.2 Atlantic Water Incursions and the Cold Halocline Layer Variability

As discussed above (Section 1.2.3), the CHL buffers the sea ice from the relatively warm AW layer below. Martinson and Steele (2001) consider ship-based observations near the North Pole, in which they find two years in which CHL is weak or absent, 1993 and 1995, and go on to calculate that the loss of the CHL buffering could result in a 70 to 80% loss in winter ice growth. Due to lack of data, they leave open the questions of how much ice loss actually occurred, and how long the CHL reduction lasted, although they do suggest a relationship between CHL loss and the phase of the AO.

Polyakov et al. (2004) argue that the Arctic is subject to large internal variability due to multi-decadal fluctuations in AW temperature and salinity. In particular, they associate the "mid-century warming" of the 1920s to the 1940s with AW inflow. The AW inflow can be associated with the high phase of the NAO but can also be independent of it, since the mid-century warming did not coincide with a positive NAO fluctuation. The time series of AW temperature is shown in Figure 8, taken from Polyakov et al. (2005). Johannessen et al. (2004) also examine the mid-century event and conclude that the warming was due to natural variability involving North Atlantic Ocean circulation. They base their conclusion on the fact that a similar event occurred in a long climate model simulation with no greenhouse gas increases. In contrast, no model simulation performed without greenhouse gas increases produced ice reductions comparable to those of the recent record. Delworth and Knutson (2000) also concluded that the mid-century warming was primarily the result of natural variability, as did a study by Wang et al. (2007) of 20th Century and preindustrial climate simulations from AR4 climate models. Polyakov et al. (2005) document an abrupt incursion of warm AW in 2004, and also point out that the warm incursion could be induced by secular climate change rather than a low-frequency fluctuation.

2.3 Evaluation of Trend Simulations for the Period of Observations

The quality of 20C3M simulations of sea ice coverage trends is assessed in studies by Zhang and Walsh (2006), Arzel et al. (2006), and Stroeve et al. (2007), of which the first two consider the annual-mean trend and the last looks specifically at the trend in September. In agreement with observations, these studies find downward trends in simulated ice cover with substantially greater loss in September than in the annual mean. For annual mean ice area, Zhang and Walsh find good agreement between the 14 model ensemble-mean trend for 1979 to 1999 and corresponding observations, with a loss rate of about 1.9% per decade for both observations and the ensemble mean (note that the rate of decline is smaller for the annual mean than it is for September coverage). The close agreement of the mean is accompanied by large ensemble spread, with an inter-model standard deviation equal to the mean trend. Of the 14 models, all but two have decreasing trends. Arzel et al. (2006) show the annual-mean trends in ice extent (as opposed to area) in the same models, and obtain essentially the same result.

Stroeve et al. (2007) found that the September extent trend in their multi-model ensemble mean was substantially smaller than the observed trend, both for the record of 1953 to 2006 and for the smaller period of satellite coverage, 1979 to 2006. In the longer period they find an ensemble-mean September trend of -2.5% per decade, compared to -7.8% for the observations, while the respective trends are -5.4% and -9.1% for the satellite period. Since the timing of the natural variability is different in each simulation, averaging across the ensemble removes most of this variability while retaining the common externally forced trend. Thus, Stroeve et al. (2007) interpret the

difference between the ensemble-mean response and the real-world trend as evidence that greenhouse gas forcing accounts for 33-38% of the half-century trend in sea ice extent and 47-57% of the stronger trend of the satellite record. They also note that external forcing might account for a larger portion of the trend, in which case the models as a group would be underestimating the sea ice reduction due to global warming. This underestimate would imply a further underestimate of the rate of future decline in the 21st Century. Stroeve et al.'s (2007) result is shown in Figure 9, which shows time series of simulated sea ice extent for the 20th and 21st century with observations. The observed September sea ice extent, shown in red, has declined faster than any of the simulations.

The results of Stroeve et al. (2007) differ from those of Zhang and Walsh and Arzel et al., who found a good match between annual-mean sea ice area trends in observations and the ensemble mean, rather than an underestimate. Further calculations by M. Holland (personal communication) show that two significant differences between the studies are the period of record and the use of sea ice extent versus sea ice area. Using the same years (1979 to 1999) and models as Zhang and Walsh, Holland found that the ensemble-mean trend in annual-mean sea ice extent was an underestimate (-2.2×10^5 km/yr for the ensemble mean, -3.5×10^5 km/yr for the observations), although the underestimate is not as severe as for the September extent trend from 1979 to 2006 considered by Stroeve et al. (2007). Like Zhang and Walsh (2006), she found that the ensemble-mean sea ice area was in good agreement with observations, although it is not clear at present why extent is underestimated for these years while area is not.

3. Projections of Future Sea Ice Loss

This section reviews studies of Arctic sea ice decline in 21st Century IPCC scenario simulations. The simplest measures are trends calculated over 100 years, discussed in section 3.1. However, as discussed in section 3.2, the 21st Century loss may not occur as a gradual, continuous decline, since the effect of natural variability can lead to abrupt loss events taking place over the course of a single decade. Finally, the relationship between the severity of future sea ice loss simulated by a climate model and the state of its sea ice in present-day simulations is reviewed in section 3.3. The association between future loss and present-day ice conditions suggests that models with better simulations of present-day conditions should be given priority in assessing the threat of future sea ice loss for polar bears.

3.1 Trends for B1, A1B, and A2 Scenarios

Climate model projections are unanimous that temperatures will continue to rise throughout the 21st Century under the influence of enhanced greenhouse gas forcing. They also agree that the warming will be largest in the high northern latitudes and will be accompanied by large reductions in Arctic sea ice, particularly at the end of the summer melt season (Meehl et al. 2007). As is the case for 20th Century simulations, agreement in the direction of the changes is accompanied by a substantial range in projections of their severity.

An examination of 21st Century trends in AR4 climate projections is provided by Zhang and Walsh (2006) and Arzel et al. (2006). Zhang and Walsh consider three different IPCC forcing scenarios, B1, A1B, and A2, in which CO_2 concentrations are controlled and stabilized at 549, 717, and 856 ppm, respectively, by the year 2100 (IPCC 2001, Appendix 2). For each scenario they calculate the decrease in

ensemble-mean summer minimum (i.e., September) ice area between 2080-2100 and 1979-1999 and obtain 45.8%, 59.7%, and 65.0% reductions for scenarios B1, A1B, and A2. They also note that no significant trends occur in an additional set of model integrations with greenhouse gas levels held fixed at year 2000 levels. As in the 20C3M simulations, they note marked inter-model diversity in the decline, with substantial overlap between the rates of decline seen in the different scenarios. In agreement with these results, Arzel et al. (2006), who consider only the A1B scenario, find a reduction in sea ice extent of 61.7% between the two periods. They further show that half of the models have an ice-free Arctic in September by 2100. This result is similar to the reduction in September ice cover found by Walsh and Timlin (2003, their Figure 5), who looked at 21st century trends in the five models considered in the Arctic Climate Impact Assessment (ACIA 2004).

3.2 Uncertainty due to Internal Variability: Abrupt Loss Events

While the studies discussed above considered only the total reduction in sea ice from the beginning to the end of the 21st Century, Holland et al. (2006b) looked in detail at the progression of the loss over the course of the century. They found that internal variability is quite important for the decade-to-decade progression of the decline. In A1B simulations performed with CCSM3 they find long-term decline punctuated by episodes of abrupt, dramatic reduction, as shown in Figure 10. In this simulation an abrupt loss event occurs over a 10-year period starting in 2024 (denoted by the grey band in fig. 10a), over which September ice retreats from 6 million km^2 to 2 million km^2. The abrupt decline is shown geographically in 10b, in which the 1990-1999 mean September sea ice extent is plotted as a black contour which contains the region in which all gridpoints have at least 50% sea ice concentration. The blue contour contains all gridpoints which have at least 50% September sea ice for the period 2010 to 2019, and it is evident that some loss has occurred between these two periods. The green contour shows September sea ice for 2040 to 2049, and the difference between the green and blue contours shows the almost complete loss of September extent associated with the abrupt transition. This rate of retreat during the abrupt loss event is three times larger than any comparable trend in observations or CCSM3 simulations for the 1979-2005 period. Episodes of abrupt reduction were found in all seven A1B simulations performed using CCSM3, occurring at various decades within the 21st Century. A further survey of A1B simulations from other climate models found comparable abrupt episodes in 6 out of 15 simulations.

The timing of the episodes in the CCSM3 simulations is immaterial for the century-long trend studied by Zhang and Walsh, since all the CCSM3 simulations lost all their September ice by the end of the century. But knowledge of the timing would be essential for any attempt at decadal prediction of the progression of the decline. Holland et al. found that abrupt loss events are preceded by pulse-like incursions of warm Atlantic water into the Arctic. The pulses are essentially the same as the AW incursions described by Polyakov et al. (2004, 2005) as a form of natural, unpredictable Arctic climate variability. Thus, even in global warming simulations in which climate change is strongly driven by external forcing, natural variability is still a prominent factor in the year-to-year and decade-to-decade changes in sea ice cover.

An interplay between forced and natural variability comes about in abrupt loss episodes through the dependence of open water formation efficiency on sea ice thickness. Open water formation efficiency is a measure of the amount of open water that forms over the course of the summertime melt season. The idea is that melting will make thick ice thinner, but the fractional ice coverage will not be affected. When the same melting occurs in thin ice, a substantial portion of the ice can melt away completely, replacing ice cover with open water.

The potential importance of open water

formation efficiency is shown in Figure 11a, which shows the decline in Arctic-averaged March sea ice thickness for the simulation in Figure 10. As one might expect, a reduction in March thickness occurs during the period of abrupt loss in areal coverage, but the thickness decline during the abrupt loss period is no greater than earlier thickness declines such as the one that occurs just prior to 2000. The amount of open water formation for the same thickness loss is much larger for thinner ice, however, as shown in Figure 11b, in which the x-axis gives the thickness of the ice and the y-axis gives the loss of ice fraction per centimeter of ice melted. Assuming that a meter of ice melts away each year during the melt season and grows back over the following winter, one would expect a loss of about 20% in ice fraction during the melt season for a region with a mean ice thickness of 3 meters. For the same meter of melting, a region with a mean thickness of 2 meters would lose about 40% of its coverage by September (the end of the melt season), and a region of 1 meter thick ice would lose all of its September ice cover.

The implication of Figure 11b for AW incursions is this: in a cold climate with predominantly thick, multi-year Arctic ice, AW incursions would occur naturally but would not have dramatic consequences for ice coverage. In a warming climate with thinner ice, the same naturally occurring AW variability would lead to substantial coverage losses. Thus, a form of natural variability can combine with greenhouse gas-induced warming to produce periods of abrupt sea ice loss. The impact of the natural variability may be further enhanced by the increased heat content of AW incursions due to the warming of the Atlantic surface waters and the amplifying effect of the sea ice-albedo feedback on open water formation. Much of the climate change literature is devoted to distinguishing between natural climate variability and forced climate change, but in this case the two act in concert, and the inherent unpredictability of natural variability leads to unpredictability in sea ice loss due to global warming.

3.3 Associations between Present-Day Simulations and Future Projections

Feedback mechanisms controlling the rate of projected sea ice decline should be somewhat dependent on the properties of the sea ice and the atmosphere (e.g. clouds) in the present-day simulation. In models with thinner ice, the higher open water formation efficiency should promote faster ice decline. In models with high summertime cloud cover one might expect the sea ice-albedo feedback to be weaker, as clouds limit the amount of sunlight absorbed by the ocean when the ice retreats. Models with less extensive ice may lose their ice more rapidly, as the ice-albedo feedback is already in operation from the start of the 21st Century simulation. Other less easily identifiable factors in the present-day simulation may be associated with future behavior, like cold biases which make the Arctic more accommodating to sea ice formation. Such associations would be of great value, since they would provide guidance for judging the credibility of future climate projections in terms of their performance in present-day simulations. As noted in section 1, sea ice simulations for present-day climate differ from model to model, and specific relationships between simulations and model formulation are not easily discovered. As in the case of present-day simulations, simulations of climate change differ for a variety of reasons, including differences in sea ice component models and the differences in the atmosphere and ocean models coupled to them. A number of physical processes determine the rate of sea ice decline, and no single property of the present-day simulation has been found to be a dominant predictor for sea ice loss in future climate projections.

Some studies report a tendency for models which have extensive ice under current conditions to lose less ice in the future. This result was found in the AR4 models by Arzel et al. (2006) and by Zhang and Walsh (2006). Zhang and Walsh also note that the relationship does not explain a large fraction of the

ensemble spread in projections of ice decline. In the five models used in the ACIA report (ACIA 2004), Walsh and Timlin (2003) found that the rate of decline does depend strongly on ice extent at the beginning of the 21st century. Flato et al. (2004) find a weakly negative relationship between present extent and future Arctic warming in the CMIP2 models, with the smaller loss for more extensive ice.

In agreement with the open water formation efficiency argument, Holland and Bitz (2003) found a relationship between ice thickness in the present and future coverage reductions. They documented this relationship in the CMIP2 models, for which Flato et al. found less Arctic warming in models with thicker present-day ice. In both studies the relationships were found to be statistically significant but not strong determinants of future behavior. Arzel et al. (2006) did not mention ice thickness in their discussion of present-future relationships in the AR4 models. Holland and Bitz examined a number of other present-day predictors, including winter cloud cover, ocean heat transport, and snow cover on land, and found statistically significant associations between these factors and simulated climate change. In all of these studies, relationships were sought between present-day predictors and climate change at the end of the 21st Century. Stronger relationships may exist for shorter term projections, say between late 20th and mid- 21st century conditions.

4. Selection Criterion for Models Used in Polar Bear Habitat Projections

Several authors have recommended using a selection criterion to choose a subset of models for use in projecting future Arctic climate, including Stroeve et al. (2007), Holland and Bitz (2003), and Wang et al. (2007). To some extent, this is simply common sense, since models which are too severely biased in the present should not be trusted for climate projections. One such model is IAP_FGOALS, which simulates ice-age like conditions for the present climate and has been identified by Zhang and Walsh (2006) as having spin-up problems. Moreover, there are relationships between present performance and future projections, as identified in the previous section. The selection criterion (or criteria) should represent a balance between the desire to focus on the most credible models and the competing desire to retain a large enough sample to assess the spread of possible outcomes.

The selection criterion used to choose an ensemble of model projections for assessing potential polar bear habitat loss is based on a modified definition of sea ice extent, in which a grid cell is considered ice-covered if its ice concentration is 50% or more. This definition is used because it has been found that polar bears do not make use of ice in areas where the concentration is less than 50% (e.g., Stirling et al. 1999, Ferguson et al. 2000, Mauritzen et al. 2003, Durner et al. 2006, 2007). Based on this modified extent, the ensemble includes only those models for which the mean 1953-1995 simulated September extent is within 20% of its observed value, which is taken from the HadISST dataset (Raynor et al. 2003). The criterion is based on Stroeve et al. (2007), who used the same averaging period and 20% threshold value, although they used the standard 15% cutoff in the definition of sea ice extent. The use of a long period of record is motivated by the desire to smooth out decadal natural variability in the definition of the climatology. One model, INMCM, has motionless sea ice and would not have been used regardless of its ice extent.

Figure 12 shows the selection of models from the set of 20 models for which sea ice concentration and thickness output were present in both the 20C3M and A1B scenarios. The A1B scenario was chosen as a representative medium-range forcing scenario, and other scenarios were not considered due to time constraints. Each model is displayed as a numbered point (1-20) on a scatter plot in which the x-axis represents mean extent in the 1953-1995 period, and the y-axis represents extent in the years 2045 to 2055 in the A1B scenario. The

vertical dashed lines on the graph represent extents 20% below and 20% above the observed climatology. Points along the green diagonal line have the same extent values for the 20th and 21st century periods. Thus, a model in which there was no loss of sea ice extent would lie on the green line. The IAP-FGOALS model (number 10) does not appear on the graph because its 20th Century extent value (19 million km^2) is well beyond the x-axis limits.

It is evident from the plot that all models have less ice in the mid-21st Century than in the 20th Century, since all points lie below the green line. Also, consistent with papers cited in section 3.3, models with extreme ice extent in 20th Century simulations lose very little ice, while models which are lacking in ice in their present-day simulations lose most or all of their ice by mid-century. The 10 models within the dashed vertical lines are the models which satisfy the selection criterion. These models show a large range of ice loss, from complete loss of September ice for CCSM3 to about 30% loss for CCCMA_CGCM. Four of the models lose over 80% of their September extent. Two of the models with the most extreme decline, CCSM3 and UKMO_HADGEM1, are cited by Stroeve et al. (2007) as having the most sophisticated sea ice component models and the best 20th Century simulations of the 18 models considered in their study. The same two models were mentioned by Gerdes and Koberle (2007) as having the most realistic sea ice thickness simulations. An examination of the September sea ice extent in the same 10 models for the period 2090 to 2099 (not shown) reveals that 7 of the models (numbers 4, 12, 14, 15, 16, 18, and 20 in fig. 12) lose over 97% of their September sea ice by the end of the 21st Century.

Sea ice projection models selected by the above criterion are used by Durner et al. (2007) to model changes in the distribution and abundance of polar bear habitat; by Hunter et al. (2007) to project trends in the Southern Beaufort Sea polar bear population, and by Amstrup et al. (2007) to project the future worldwide polar bear population.

5. Concluding Remarks

Climate model simulations are in universal accord that greenhouse gas increases will cause Arctic sea ice cover to decline, with the greatest reductions occurring at the end of the summer melt season. The physical principles underlying this behavior are simple and well established: the decline is a consequence of the heat-trapping effect of greenhouse gases and the inherent sensitivity of sea ice to a warming climate, particularly due to the sea ice-albedo feedback. A further consistency in climate simulations is the uneven latitudinal distribution of global warming, which always has its greatest simulated impact in the high northern latitudes. This "polar amplification" and associated sea ice decline have been consistent climate simulation features at least since the early simulation of Manabe and Souffer (1980). Since Chapman and Walsh (1993), declines in Arctic sea ice, with the largest trends in September, have also been consistently reported in observations (see references in Serreze and Francis 2005).

In simulations by all generations of models, agreement in direction has been accompanied by a large range in projections of the severity of the decline, as can be seen in Figure 12. These differences are a consequence of differences in model formulation and, perhaps to a lesser extent, to the unpredictable natural variability in the simulations. Formulation differences are differences in discretization, resolution, and the representation of unresolved processes through parameterization. Uncertainties in climate simulation necessitate the use of ensembles of simulations from several models, from which the range of possible outcomes can be appreciated. Often the average across the ensemble is in reasonable agreement with observations despite the large spread of the ensemble, as is the case with the ensemble median sea ice edge (Flato et al. 2004; Arzel et al. 2006; Zhang and Walsh 2006).

On a more fundamental level, the presence of uncertainty in climate simulations is an inevitable consequence of the underlying

sensitivity of the climate system. Any feedback mechanism which serves to amplify the climate change produced by greenhouse gases is also likely to amplify the model-to-model differences caused by parameterization choices. As an important example, sea ice-albedo feedback makes sea ice extent sensitive to changes in greenhouse gases because reductions in ice cover lead to more absorption of sunlight by the ocean, leading to further sea ice melting. This feedback process will also operate if the initial sea ice reduction is brought about by a change in the parameterization of clouds or upper ocean turbulent mixing, or any other unresolved process that affects sea ice. The close association between uncertainty and climate sensitivity suggests that future climate projections will always be expressed in terms of a range of outcomes. Uncertainty does not arise because the models are bad, but because the climate system is sensitive. The most dramatic forms of climate change, sea ice decline in particular, will always be the most difficult to simulate.

Unpredictable internal variability also complicates attempts to make future climate projections and to verify climate simulations against observations. One might expect the verification problem to go away over time, as the forced climate change becomes larger and rises above the "noise" of natural variability. However, studies like Holland et al. (2006b) suggest that natural variability will continue to be an integral part of the Arctic climate problem. Climate simulations typically show smooth increases in global temperature in response to smoothly increasing levels of well-mixed greenhouse gases. But Holland et al.'s (2006b) results show abrupt reductions in sea ice despite the smoothness of the external forcing. The abrupt loss events are triggered by apparently random Atlantic water incursions not directly related to the external forcing. The implication is that climate variability will always be a complicating factor in understanding climate change, and the consequent unpredictability will always be a confounding factor in attempts to anticipate sea ice decline.

This document gives an overview of the reasons for uncertainty in climate model projections of Arctic sea ice decline. Perhaps the most important lesson from the extensive history of climate projections is that uncertainty, both in model construction and from internal variability, is an essential ingredient of the climate change problem. We anticipate that future generations of climate model projections will continue to produce a substantial range of estimates of the pace of sea ice loss. As with present models, the best guidance from these models will come from selective subsets, using the ensemble mean as the best estimate and the ensemble spread to cover the probable range of outcomes. The recent climateprediction.net study by Knutti et al. (2006, see section 1.3 above) suggests that it is difficult to assign an upper bound to the global temperature increase which could occur due to increased CO_2. In that case, the range of estimates of Arctic sea ice decline examined here may also be too conservative. While quantitative estimates of the range of likely outcomes cannot be easily obtained, evidence from model simulations, consistent with the recent trend in observations, suggests a dramatic loss in September sea ice cover over the 21st Century.

Summary of Key Points

Some key points of this report are listed below:

1. Sensitivity and uncertainty go hand in hand. The same factors which make Arctic sea ice susceptible to rapid loss under global warming also make sea ice difficult to simulate. For this reason, projections of Arctic sea ice loss will always be expressed in terms of a range of likely estimates, rather than precise predictions of the timing and severity of the loss.
2. Climate models are capable of simulating the gross features of sea ice, including annual means and seasonal cycles of sea ice area and extent.
3. The models also simulate the recent decreasing trends in area and extent of sea ice, although the September extent trend is underestimated. The implication is that, if anything, models may be too conservative in their estimates of the rate of future decline.
4. Sea ice decline in future projections is linked to the present-day sea ice simulation. Thus, a selection criterion based on present-day model performance should be used to choose a subset of models for use in considerations of future polar bear habitat loss.
5. Unpredictable natural variability will always confound attempts to make precise forecasts of sea ice decline. Natural variability can combine with greenhouse gas-induced climate change to produce periods of rapid sea ice loss.
6. For the A1B scenario, all models considered here simulate declines of September Arctic sea ice extent over the 21st century. Of models which satisfy the selection criterion described in section 4, all show declines of over 30% by the middle of the 21st Century, and 4 of 10 models have declines in excess of 80%. Seven of the ten models lose all their September sea ice by the end of the century.

Acknowledgements

I thank Cecillia Bitz and John Walsh for their insightful reviews of a draft of this report. Consultations with Marika Holland, Xiangdong Zhang, and Julienne Stroeve were also valuable in understanding the results of their research. My research on the simulation of the Arctic in climate models is supported by the U.S. Department of Energy through grant DE-FG02-03ER63604.

References Cited

Achuta Rao, K., C. Covey, C. Doutriaux, M. Fiorino, P. Gleckler, T. Phillips, K. Sperber, and K. Taylor. 2004. Appraisal of coupled climate model simulations. Lawrence Livermore National Laboratory, California, Report UCRL-TR-202550.

ACIA. 2004. Arctic Climate Impact Assessment: Scientific Report. Cambridge University Press, United Kingdom.

Alley, R.B., W.D. Nordhaus, J.T. Overpeck, D.M. Peteet, R.A. Pielke, Jr., R.T. Pierrehumbert, P.B. Rhines, T.F. Stocker, L.D. Talley, and J.M. Wallace. 2003. Abrupt climate change. Science 299:2005-2010.

Amstrup, S.A. 2003. Polar bear, *Ursus maritimus*. Pages 587-610 in G.A. Feldhamer, B.C. Thompson, and J.A. Chapman (Editors). Wild Mammals of North America: Biology, Management, and Conservation. Johns Hopkins University Press, Baltimore, Maryland, 2nd edition.

_____, B.G. Marcot, and D.C. Douglas. 2007. Forecasting the Rangewide Status of Polar Bears at Selected Times in the 21st Century. USGS Alaska Science Center, Anchorage, Administrative Report.

Arzel, O., T. Fichefet, and H. Goosse. 2006. Sea ice evolution over the 20th and 21st centuries as simulated by current AOGCMs. Ocean Modelling 12:401-415.

Beesley, J.A., and R.E. Moritz. 1999. Toward an explanation of the annual cycle of cloudiness over the Arctic Ocean. Journal of Climate 12:395-415.

Bitz, C.M., G. Flato, and J. Fyfe. 2002. Sea ice response to wind forcing from AMIP models. Journal of Climate 15:523-535.

_____, M.M. Holland, A.J. Weaver, and M. Eby. 2001. Simulating the ice-thickness distsribution in a coupled climate model. Journal of Geophysical Research 106C: 2441-2463.

_____, and G.H. Roe. 2004. Mechanism for the high rate of sea ice thinning in the Arctic Ocean. Journal of Climate 17:3622-3631.

Boville, B.A., P.J. Rasch, J.J. Hack, and J.R. McCaa. 2006. Representation of clouds and precipitation processes in the Community Atmosphere Model Version 3 (CAM3). Journal of Climate 19:2184-2198.

Cavalieri, D.J., C.L. Parkinson, P. Gloersen, J.C. Comiso, and H.J. Zwally. 1999. Deriving long-term time series of sea ice cover from satellite passive-microwave multisensor data sets. Journal of Geophysical Research 104(C7):15,803-15,814.

Chapman, W.L., and J.E. Walsh. 1993. Recent variations of sea ice and air temperatures in high latitudes. Bulletin of the American Meteorological Society 74:33-47.

_____, and _____. 2007. Simulation of Arctic temperature and pressure by global coupled models. Journal of Climate 20:609-632.

Collins, W.D., C.M. Bitz, M.L. Blackmon, G.B. Bonan, C.S. Bretherton, J.A. Carton, P. Chang, S.C. Doney, J.J. Hack, T.B. Henderson, J.T. Kiehl, W.G. Large, D.S. McKenna, B.D. Santer, and R.D. Smith. 2006. Community Climate System Model Version 3 (CCSM3). Journal of Climate 19:2122-2143.

Delworth, T.L., and T.R. Knutson. 2000. Simulation of early 20th Century global warming. Science 287:2246-2250.

Deser, C., and J.E. Timlin. 2000. Arctic sea ice variability in the context of recent atmospheric circulation trends. Journal of Climate 13:617-633.

DeWeaver, E., and C.M.Bitz. 2006. Atmospheric circulation and its effect on Arctic sea ice in CCSM3 simulations at medium and high resolution. Journal of Climate 19:2415-2436.

_____, M.M. Holland, and E.C. Hunke. 2007. Comment on Eisenman et al., "On the reliability of simulated Arctic sea ice in global climate models." Geophysical Research Letters: Submitted.

Durner, G.M., D.C. Douglas, R.M. Nielson, and S.C. Amstrup. 2006. Model for Autumn Pelagic Distribution of Adult Female Polar Bears in the Chukchi Seas, 1987-1994. USGS Alaska Science Center, Anchorage, Final Report to USFWS.

_____, _____, _____, _____, and T.L. McDonald. 2007. Predicting the Future Distribution of Polar Bear Habitat in the Polar Basin from Resource Selection Functions Applied to 21st Century General Circulation Model Projections of Sea Ice. USGS Alaska Science Center, Anchorage, Administrative Report.

Ebert, E.E., and J.A. Curry. 1993. Intermediate one-dimensional thermodynamic sea ice model for investigating ice-atmosphere interactions. Journal of Geophysical Research 98(C6):10,085-10,109

Eisenman I., N. Untersteiner, J.S. Wettlaufer. 2007. On the reliability of simulated Arctic sea ice in global climate models, Geophysical Research Letters 34:L10501.

Ferguson, S.H., M.K. Taylor, and F. Messier. 2000. Influence of sea ice dynamics on habitat selection by polar bears. Ecology 81:761-772.

Fischbach, A.S., S.C. Amstrup, and D.C. Douglas. 2007. Landward and eastward shift

of Alaskan polar bear denning associated with recent sea ice changes. Polar Biology:in press.

Flato, G.M., and participating CMIP Modeling Groups. 2004. Sea ice and its response to CO_2 forcing as simulated by global climate models. Climate Dynamics 23:229-241.

Gerdes, R., and C. Koberle. 2007. Comparison of Arctic sea ice thickness variability in IPCC climate of the 20th Century experiments and in ocean-sea ice hindcasts. Journal of Geophysical Research 112(C4):C04S13.

Gorodetskaya, I.V., L.-B. Tremblay, B. Liepert, M.A. Cane, and R.I. Cullather. 2007. Modification of the Arctic Ocean short-wave radiation budget due to cloud and sea ice properties in coupled models and observations. Journal of Climate:in press.

Hack, J.J., J.M. Caron, G. Danabasoglu, K.W. Oleson, C.M. Bitz, and J.E. Truesdale. 2006. CCSM-CAM3 climate simulation sensitivity to changes in horizontal resolution. Journal of Climate 19:2267-2289.

Hall, A., and X. Qu. 2006. Using the current seasonal cycle to constrain snow albedo feedback in future climate change. Geophysical Research Letters 33:L03502.

Hibler, W.D., III. 1979. Dynamic thermodynamic sea ice model. Journal of Physical Oceanography 9:815-846.

_____, and G.M. Flato. 1992. Sea ice models. In K.E. Trenberth (Editor). Climate System Modeling. Cambridge University Press, United Kingdom.

Holland, M.M., and C.M. Bitz. 2003. Polar amplification in climate models. Climate Dynamics 21:221-232.

_____, _____, E.C. Hunke, W.H. Lipscomb, and J.L. Schramm. 2006. Influence of the sea ice thickness distribution on polar climate in CCSM3. Journal of Climate 19:2398-2414.

_____, _____, and B. Tremblay. 2006. Future abrupt reductions in the summer Arctic sea ice. Geophysical Research Letters 33:L23503.

Hunke, E.C., and J.K. Dukowicz. 1997. Elastic-viscous-plastic model for sea ice dynamics. Journal of Physical Oceanography 27:1849-1867.

Hunter, C.M., H. Caswell, M.C. Runge, S.C. Amstrup, E.V. Regehr, and I. Stirling. 2007. Polar Bears in the Southern Beaufort Sea II: Demography and Population Growth in Relation to Sea Ice Conditions. USGS Alaska Science Center, Anchorage, Administrative Report.

Hurrell, J.W. 1995. Decadal trends in the North Atlantic Oscillation. Science 269:676-679.

IPCC. 2001. Climate Change: The Scientific Basis. Contribution of Working Group I to the 3rd Assessment Report of the IPCC. Cambridge University Press, United Kingdom.

Johannessen, O.M., L. Bengtsson, M.W. Miles, S.I. Kuzmina, V.A. Semenov, G.V. Alekseev, A.P. Nagurnyi, V. Zakharov, L.P. Bobylev, L.H. Pettersson, K. Hasselmann, and H.P. Cattle. 2004. Arctic climate change: Observed and modelled temperature and sea-ice variability. Tellus 56A:328-341.

Kattsov, V.M., E. Kallen, and coauthors. 2005. Future climate change: modeling and scenarios for the Arctic. Chapter 4 in Arctic Climate Impact Assessment. Cambridge University Press, United Kingdom.

Knutti, R., G.A. Meehl, M.R. Allen, and D.A. Staniforth. 2006. Constraining climate sensitivity from the seasonal cycle in surface temperature. Journal of Climate 19(17):4224-4233.

Koberle, C., and R. Gerdes. 2003. Mechanisms determining the variability of Arctic sea ice conditions and export. Journal of Climate 16:2843-2858.

Limpasuvan, V., and D.L. Hartmann. 2000. Wave-maintained annular modes of climate variability. Journal of Climate 13:4414-4429.

Lindsay, R.W., and J. Zhang. 2005. Thinning of

Arctic sea ice, 1988-2003: Have we passed a tipping point? Journal of Climate 18:4879-4894.

Manabe, S., and R.J. Stouffer. 1980. Sensitivity of a global climate model to an increase of CO_2 concentration in the atmosphere. Journal of Geophysical Research 85(C10):5529-5554.

Martinson, D.G., and M. Steele. 2001. Future of the Arctic sea ice cover: Implications of an Antarctic analogue. Geophysical Research Letters 28:307-310.

Mauritzen, M., S.E. Belikov, A.N. Boltunov, A.E. Derocher, E. Hansen, R.A. Ims, O. Wiig, and N. Yoccoz. 2003. Functional responses in polar bear habitat selection. Oikos 100:112-124.

Maykut, G.A., and N. Untersteiner. 1971. Some results from a time-dependent thermodynamic model of sea ice. Journal of Geophysical Research 76:1550-1575.

Meehl, G. 1992. Global coupled models: Atmosphere, ocean, sea ice. In K.E. Trenberth (Editor). Climate System Modeling. Cambridge University Press, United Kingdom.

_____, C. Covey, B. McAvaney, M. Latif, and R. Stouffer. 2005. Overview of the coupled model intercomparison project. Bulletin of the American Meteorological Society 86:89-93.

_____, T.F. Stocker, W.D. Collins, P. Friedlingstein, A.T. Gaye, J.M. Gregory, A. Kitoh, R. Knutti, J.M. Murphy, A. Noda, S.C.B. Raper, I.G. Watterson, A.J. Weaver, and Z.-C. Zhao. 2007. Global Climate Projections. In S. Solomon, D. Qin, M. Manning, and H.L. Miller (Editors). In Climate Change 2007: The Physical Science Basis. Contribution of Working Group I to the 4th Assessment Report of the IPCC. Cambridge University Press, United Kingdom. Available from *http://www.ipcc.ch/*.

Obbard, M.E., M.R.L. Cattet, T. Moddy, L.R. Walton, D. Potter, J. Inglis, and C. Chenier. 2006. Temporal trends in the body condition of southern Hudson Bay polar bears. Climate Change Research Information Note 3:1-8. Available from *http://sit.mnr.gov.on.ca*.

Osterkamp, T.E., and V.E. Romanovsky. 1999. Evidence for warming and thawing of discontinuous permafrost in Alaska. Permafrost Processes 10:17-37.

Overland, J.E., and M. Wang. 2005. Arctic climate paradox: The recent decrease of the Arctic Oscillation. Geophysical Research Letters 32:L06701.

Parkinson, C.L., and W.M. Washington. 2005. Introduction to Three-dimensional Climate Modeling. University Science Books, Herndon, Virginia.

_____, K.Y. Vinnikov, and D.J. Cavalieri. 2006a. Evaluation of the simulation of the annual cycle of Arctic and Antarctic sea ice coverages by 11 major global climate models. Journal of Geophysical Research 111:C07012.

_____, _____, and _____. 2006b. Correction to "Evaluation of the simulation of the annual cycle of Arctic and Antarctic sea ice coverages by 11 major climate models." Journal of Geophysical Research 111:C12009.

Polyakov, I., G.V. Alekseev, L.A. Timokhov, U.S. Bhatt, R.L. Colony, H.L. Simmons, D. Walsh, J.E. Walsh, and V.F. Zakharov. 2004. Variability of the intermediate Atlantic water of the Arctic Ocean over the last 100 years. Journal of Climate 17:4485-4497.

_____, A. Beszczynska, E. Carmack, I.A. Dmitrenko, E. Fahrbach, I.E. Frolov, R. Gerdes, E. Hansen, J. Holfort, V.V. Ivanov, M.A. Johnson, M. Karcher, F. Kauker, J. Morison, K.A. Orvik, U. Schauer, H.L. Simmons, O. Skagseth, V.T. Sokolov, M. Steele, L.A. Timokhov, D. Walsh, and J.E. Walsh. 2005. One more step toward a warmer Arctic. Geophysical Research Letters 32:L17605.

Proshutinsky, A., M. Steele, J. Zhang, G.

Holloway, N. Steiner, S. Häkkinen, D.M. Holland, R. Gerdes, C. Koeberle, M. Karcher, M. Johnson, W. Maslowski, Y. Zhang, W. Hibler, and J. Wang. 2001. Arctic Ocean Model Intercomparison Project (AOMIP). Eos 82(51):637-644

Quadfasel, D.A., A. Sy, D. Wells, and A. Tunik. 1991. Warming in the Arctic. Nature 350:385.

Randall, D.A., R.A. Wood, S. Bony, R. Colman, T. Fichefet, J. Fyfe, V. Kattsov, A. Pitman, J. Shukla, J. Srinivasan, R.J. Stouffer, A. Sumi, and K.E. Taylor. 2007. Climate models and their evaluation. In S. Solomon, D. Qin, M. Manning, and H.L. Miller (Editors). In Climate Change 2007: The Physical Science Basis. Contribution of Working Group I to the 4th Assessment Report of the IPCC. Cambridge University Press, United Kingdom. Available from *http://www.ipcc.ch/*.

Randall, D.M., J. Curry, D. Battisti, G. Flato, R. Grumbine, S. Hakkinen, D. Martinson, R. Preller, J. Walsh, and J. Weatherly. 1997. Status and outlook for large-scale modeling of atmosphere-ice-ocean interactions in the Arctic. Bulletin of the American Meteorological Society 79:197-219.

Raynor, N.A., D.E. Parker, E.B. Horton, C.K. Folland, V.L. V. Alexander, and D.P. Rowell. 2003. Global analyses of sea surface temperature, sea ice, and night marine air temperature since the late nineteenth century. Journal of Geophysical Research 108(D14):4407.

Regehr, E.V., Amstrup, S.C., and Stirling, I. 2006. Polar Bear Population Status in the Southern Beaufort Sea. USGS Alaska Science Center, Anchorage, Open File Report 1337.

Richter-Menge, J., J. Overland, A. Proshutinsky, V. Romanovsky, L. Bengtsson, L. Brigham, M. Dyurgerov, J. C. Gascard, S. Gerland, R. Graversen, C. Haas, M. Karcher, P. Kuhry, J. Maslanik, H. Melling, W. Maslowski, J. Morison, D. Perovich, R. Przybylak, V. Rachold, I. Rigor, A. Shiklomanov, J. Stroeve, D. Walker, and J. Walsh. 2006. State of the Arctic Report. NOAA/OAR/PMEL, Seattle, Washington, Special Report.

Rigor, I.G., and J.M. Wallace. 2004. Variations in age of Arctic sea ice and summer sea-ice extent. Geophysical Research Letters 31:L09401.

_____, _____, and R.L. Colony. 2002. Response of sea ice to the Arctic Oscillation. Journal of Climate 15:2648-2663.

Rind, D., R. Healy, C. Parkinson, and D. Martinson. 1995. Role of sea ice in 2x CO_2 climate model sensitivity. Part I: The total influence of sea ice thickness and extent. Journal of Climate 8:449-463.

Rothrock, D.A., and J. Zhang. 2005. Arctic Ocean sea ice volume: What explains its depletion? Journal of Geophysical Research 110:C01002.

Semtner, A.J., Jr. 1976. Model for the thermodynamic growth of sea ice in numerical investigations of climate. Journal of Physical Oceanography 6:379-389.

Serreze, M.C., and J.A. Francis. 2005. Arctic amplification debate. Climatic change 76(3/4):241-264.

_____, M.M. Holland, and J. Stroeve. 2007. Perspectives on the Arctic's shrinking sea-ice cover. Science 315:1533-1536.

Shaw, G.E. 1995. Arctic haze phenomenon. Bulletin of the American Meteorological Society 76:2403-2413.

Solomon, S., D. Qin, M. Manning, Z. Chen, M. Marquis, K.B. Averyt, M. Tignor, and H.L. Miller (Editors). 2007. Summary for policymakers. In Climate Change 2007: The Physical Science Basis. Contribution of Working Group I to the 4th Assessment Report of the Intergovernmental Panel on Climate Change (IPCC). Cambridge University Press, United Kingdom. Available from *http://www.ipcc.ch/*.

Somerville, R.H., H. Le Treut, U. Cubash, U. Ding, C. Mauritzen, A. Mokssit, T. Peterson,

and M. Prather. 2007. Historical overview of climate change. In S. Solomon, D. Qin, M. Manning, and H.L. Miller (Editors). In Climate Change 2007: The Physical Science Basis. Contribution of Working Group I to the 4th Assessment Report of the IPCC. Cambridge University Press, United Kingdom. Available from *http://www.ipcc.ch/*.

Stirling, I., N.J. Lunn, and J. Iacozza. 1999. Long-term trends in the population ecology of polar bears in western Hudson Bay in relation to climate change. Arctic 52:294-306.

_____, and C.L. Parkinson. 2006. Possible effects of climate warming on selected populations of polar bears (*Ursus maritimus*) in the Canadian Arctic. Arctic 59:261-275.

Stroeve J., M.M. Holland, W. Meier, T. Scambos, and M. Serreze. 2007. Arctic sea ice decline: Faster than forecast. Geophysical Research Letters 34:L09501.

Thompson, D.W.J., and J.M. Wallace. 2000. Annular modes in the extratropical circulation. Part I: Month-to-month variability. Journal of Climate 13:1018-1036.

_____, _____, and G.C. Hegerl. 2000. Annular modes in the extratropical circulation. Part II: Trends. Journal of Climate 13:1000-1016.

Thorndike, A.S., D.A. Rothrock, G.A. Maykut, and R. Colony. 1975. Thickness distribution of sea ice. Journal of Geophysical Research 80(C33):4501-4513.

Tremblay, L.-B., M.M. Holland, I.V. Gorodetskaya, and G.A. Schmidt. 2007. Ice-free Arctic? Computing in Science and Engineering 9:65-74.

Uttal, T., J.A. Curry, M.G. McPhee, D.K. Perovich, R.E. Moritz, J.A. Maskanik, P.S. Guest, H.L. Stern, J.A. Moore, R. Turenne, A. Heiberg, M.C. Serreze, D.P. Wylie, O.G. Persson, C.A. Paulson, C. Halle, J.H. Morison, P.A. Wheeler, A. Makshtas, H. Welch, M.D. Shupe, J.M. Intrieri, K. Stamnes, R.W. Lindsay, R. Pinkel, W.S. Pegau, T.P. Stanton, and T.C. Grenfeld. 2002. Surface heat budget of the Arctic Ocean. Bulletin of the American Meteorological Society 83:255-275.

Vavrus, S.J. 2004. Impact of cloud feedbacks on Arctic climate under greenhouse forcing, Journal of Climate 17:603-615.

Walsh, J.E., V.M. Kattsov, W.L. Chapman, V. Govorkova, and T. Pavlova. 2002. Comparison of Arctic climate simulations by uncoupled and coupled global models. Journal of Climate 15:1429-1446.

_____, and M.S. Timlin. 2003. Northern Hemisphere sea ice simulations by global climate models. Polar Research 22:75-82.

Wang, M., and J.E. Overland. 2005. Detecting Arctic climate change using Koppen climate classification. Climatic Change 67:43-62.

_____, _____, V. Kattsov, and T. Pavlova. 2007. Intrinsic versus forced variability in coupled climate model simulations over the Arctic during the twentieth century. Journal of Climate 20:1093-1107.

Zhang, X., and J.E. Walsh. 2006. Toward a seasonally ice-covered Arctic Ocean: Scenarios from the IPCC AR4 model simulations. Journal of Climate 19:1730-1747.

Zhang, Y., W. Maslowski, and A.J. Semtner. 1999. Impact of mesoscale ocean currents on sea ice in high-resolution Arctic ice and ocean simulations. Journal of Geophysical Research 104(C8):18,409-18,429.

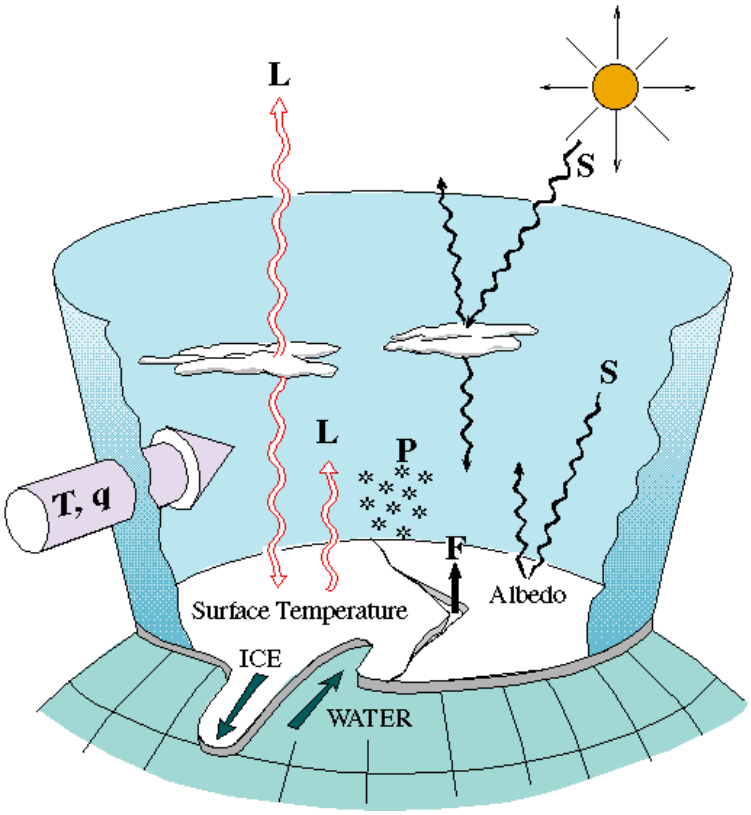

Figure 1. Schematic of physical processes which determine the heat input to Arctic sea ice.

The figure shows the longwave radiation (L) emitted by clouds and the surface, the solar radiation (S) received at the surface, some of which is reflected away due to the high albedo (i.e. reflectivity) of ice and snow, and some of which is reflected or transmitted by clouds. Heat energy is also lost through heat and moisture fluxes (F) from the surface to the overlying atmosphere, particularly at leads, and the polar cap gains heat energy from lower latitudes through northward transport of relatively warm, moist air masses (T,q). Taken from the prospectus of the Surface Heat Budget of the Arctic experiment.

Figure 2: Aerial view of the Canadian Coast Guard Ship Des Groseilliers during the Surface Heat Budget of the Arctic field experiment, August 3, 1998.

Light blue areas are melt ponds on the ice surface, darker regions are open ocean. Photo by Sylvie Lemelin, CCG.

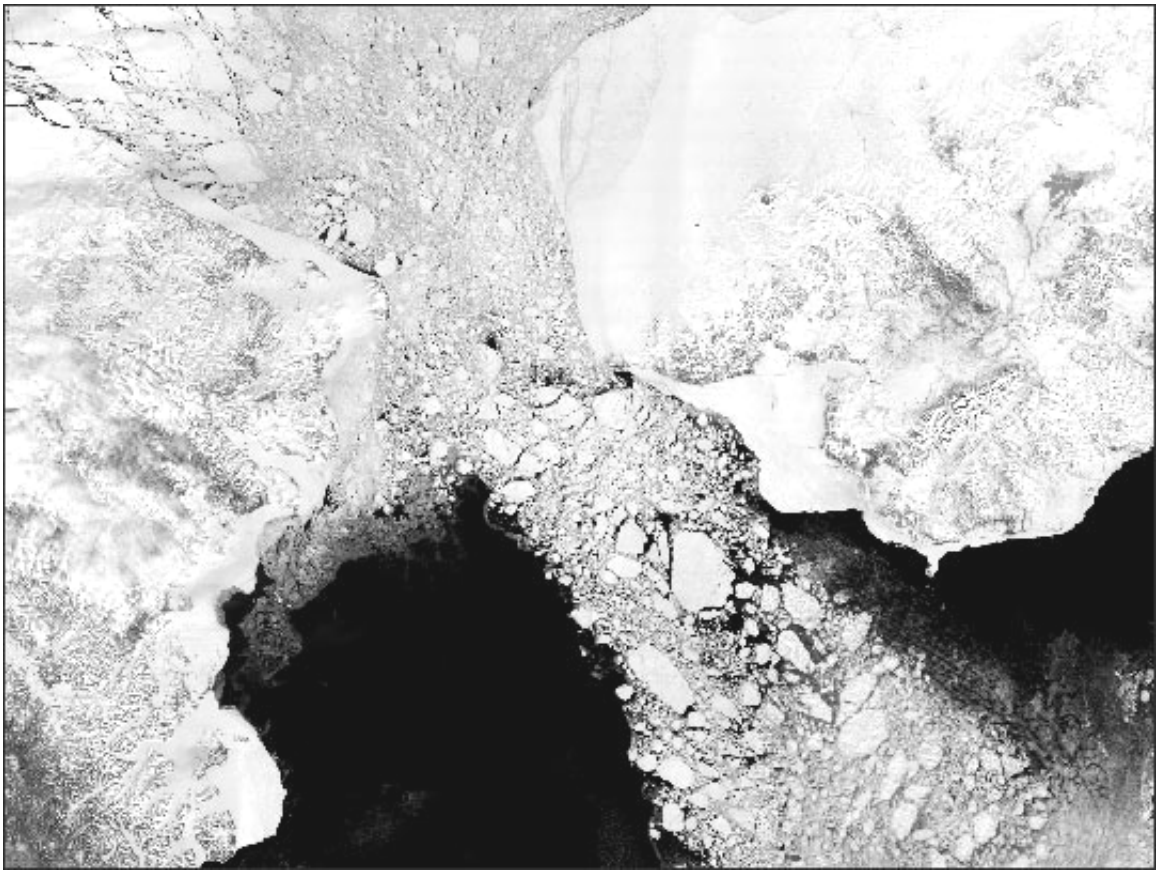

Figure 3: Sea ice in the Bering Strait, as seen by the MODIS instrument aboard the TERRA satellite, May 7, 2000.

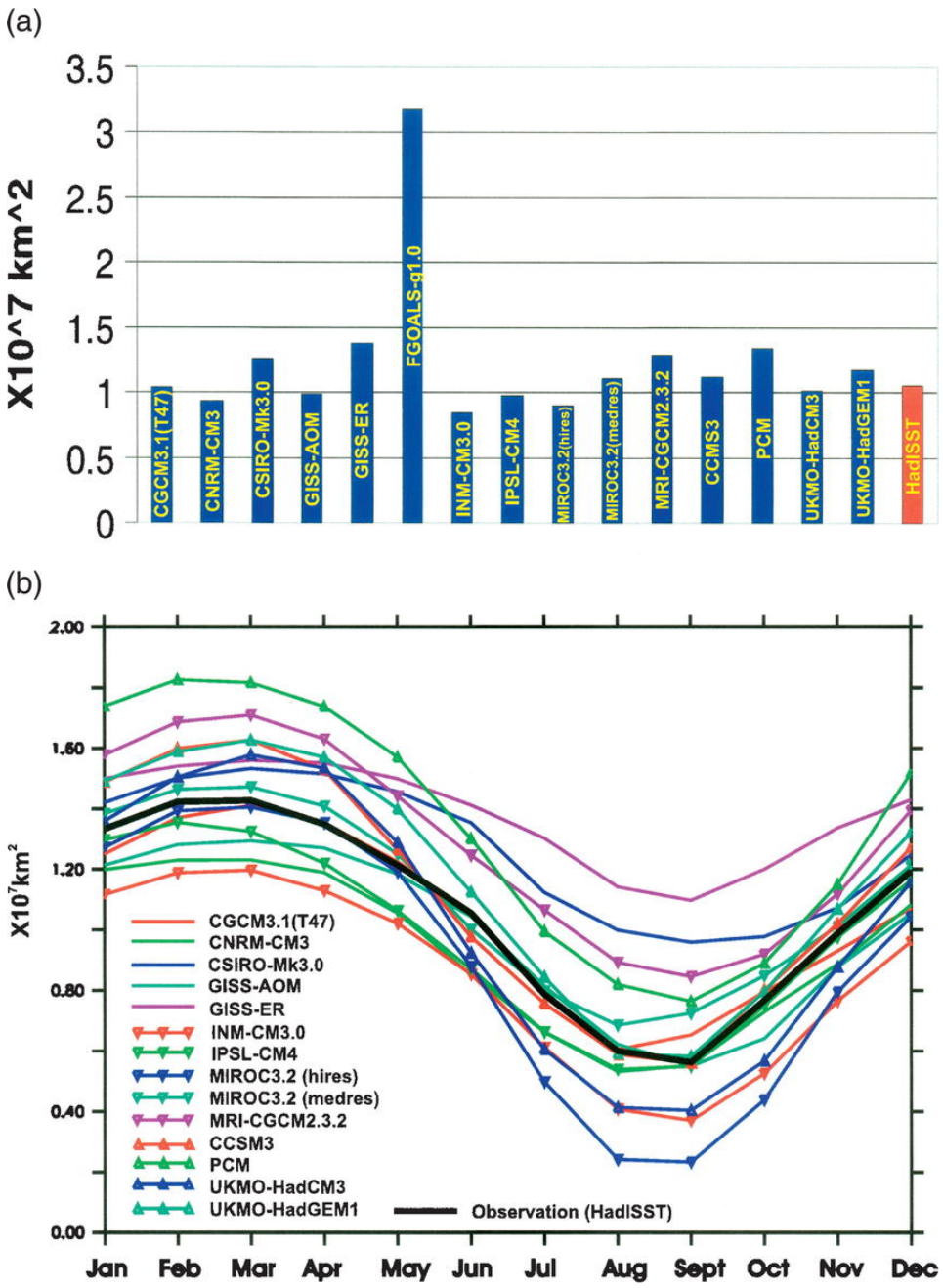

Figure 4: Climatological (a) annual mean and (b) seasonal cycles of sea ice areas during 1979–99 over the Northern Hemisphere from 15 IPCC AR4 models in the 20C3M simulations and from the HadISST1 observational analysis data. From Zhang and Walsh (2006).

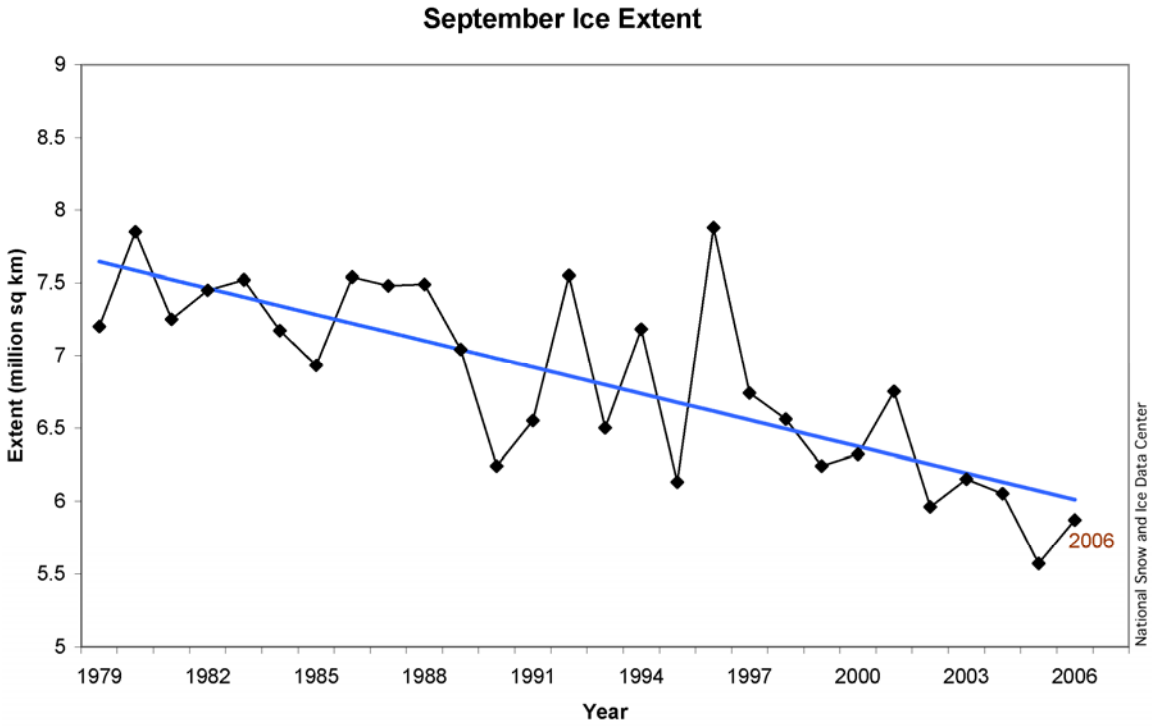

Figure 5: September Arctic sea ice extent, 1979 to 2006, from the website of the National Snow and Ice Data Center (http://www.nsidc.org).

As of 28 August 2007, with the melt season still in progress, sea ice extent has fallen to 4.78 million km^2.

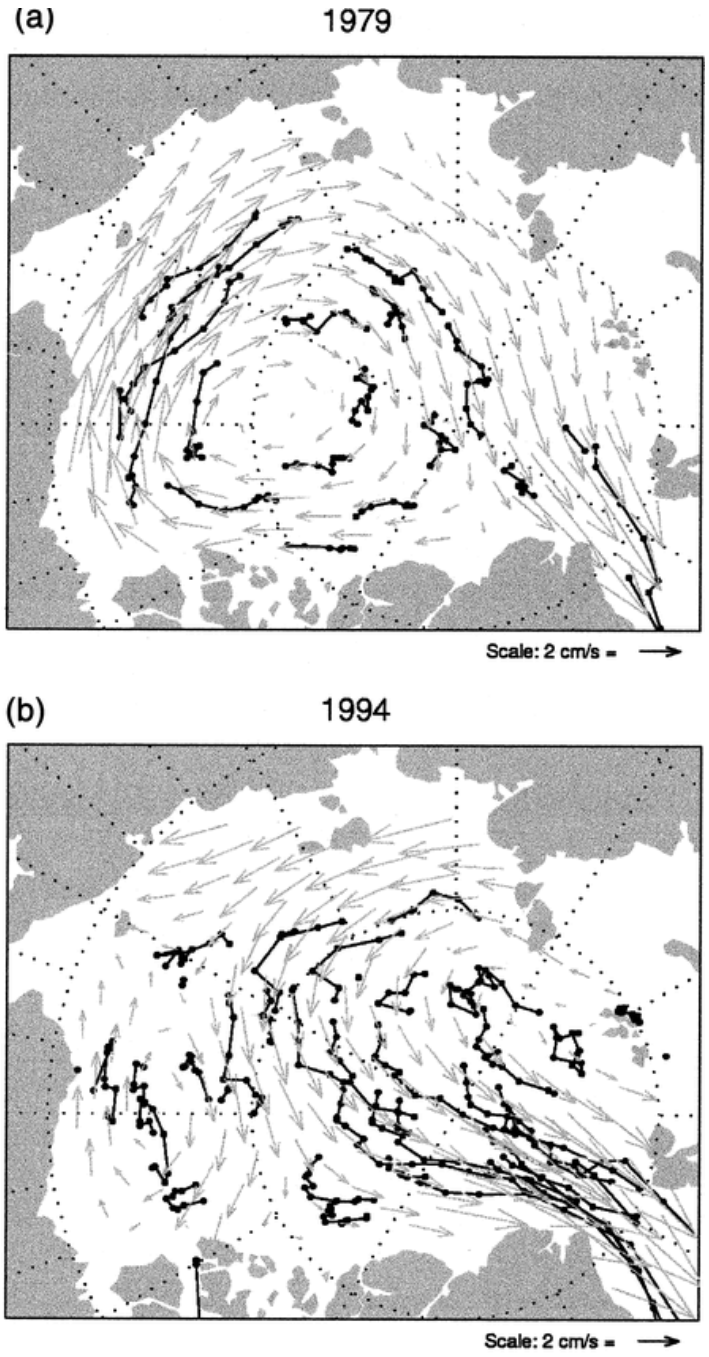

Figure 6: Patterns of sea ice motion for (a) 1979 and (b) 1994 (gray vectors).

The monthly positions of the buoys are also shown. Trajectories of individual buoys from the International Arctic Buoy Program are indicated by black lines. From Rigor et al. (2002).

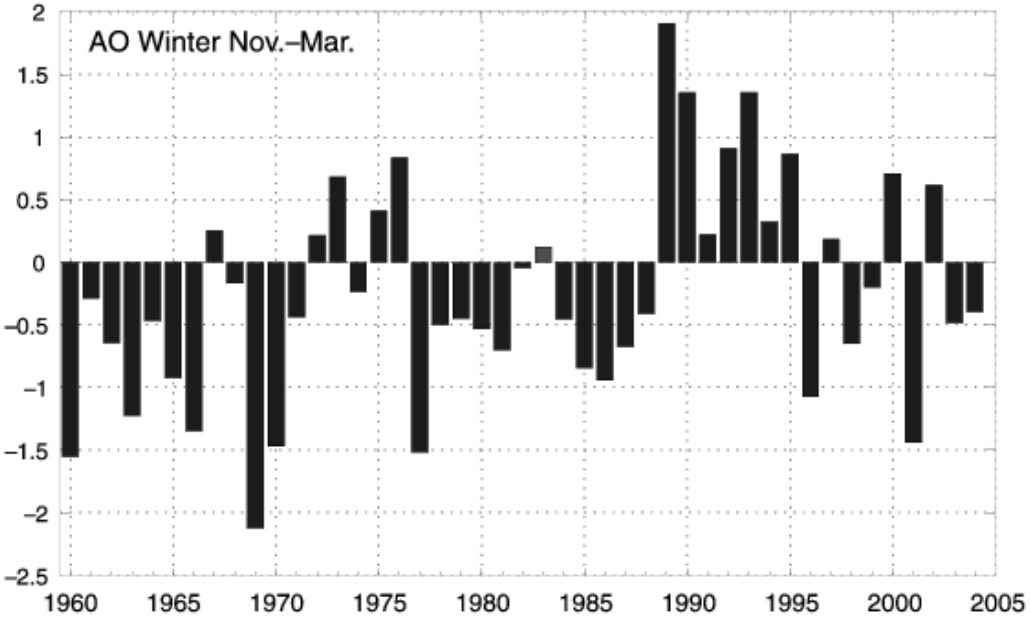

Figure 7: Time series of winter (November to March) Arctic Oscillation index. Data are from the Climate Prediction Center (CPC). From Overland and Wang (2005).

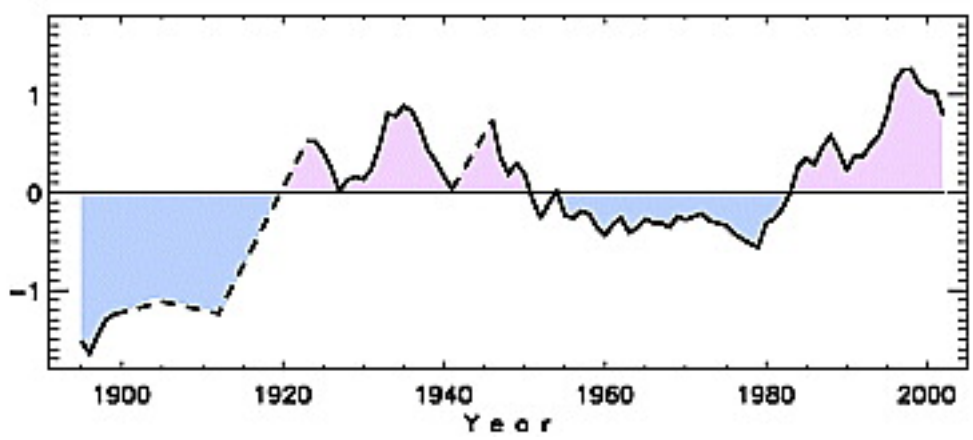

Figure 8: Long-term variability of temperature of the intermediate Atlantic water (AW) layer in the Arctic Ocean. Prolonged warm (red shade) and cold (blue shade) periods associated with phases of multi-decadal variability and a background warming trend are apparent from the record of 6-year running mean normalized AW temperature anomalies (dashed segments represent gaps in the record).

From Polyakov et al. (2005).

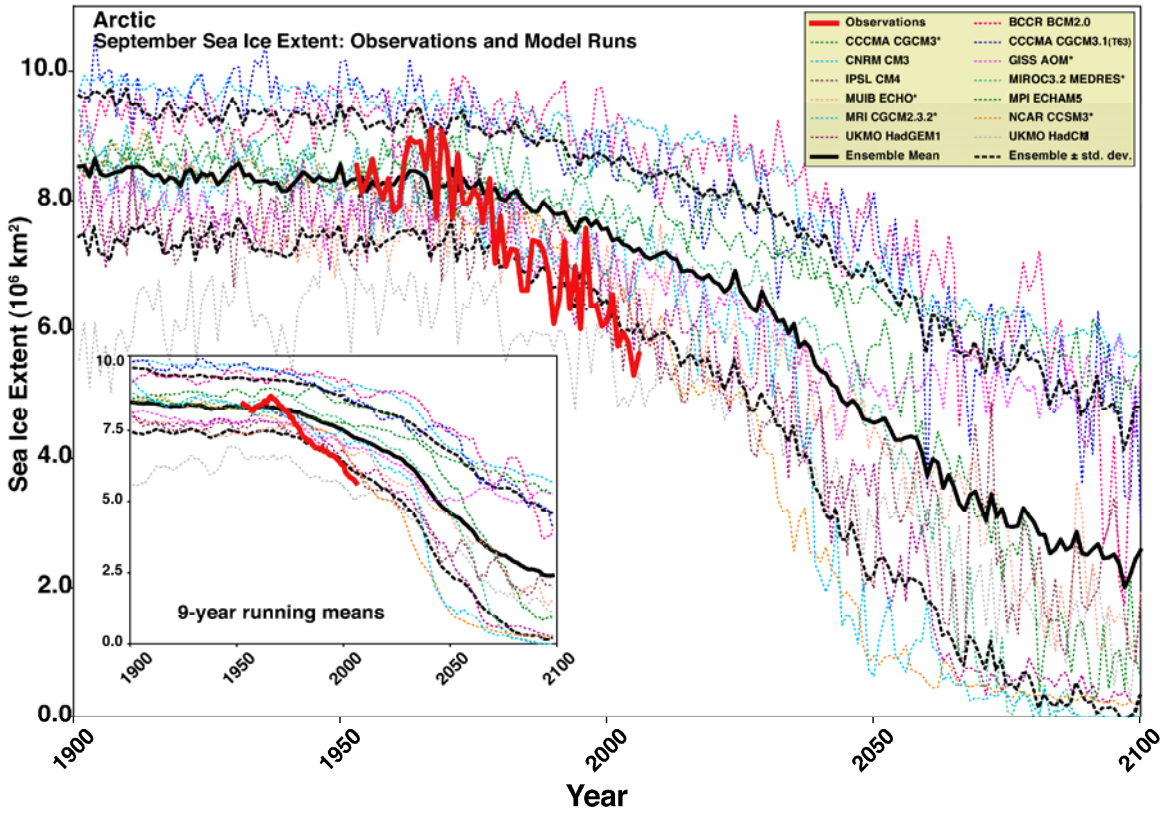

Figure 9: September Arctic sea ice extent (in millions of square kilometers) from observations (thick red line) and 13 IPCC AR4 climate models, together with the multi-model ensemble mean (solid black line) and standard deviation (dotted black line).

The 21st century values are from simulations of the A1B scenario. Inset shows 9-yr running means. From Stroeve et al. (2007).

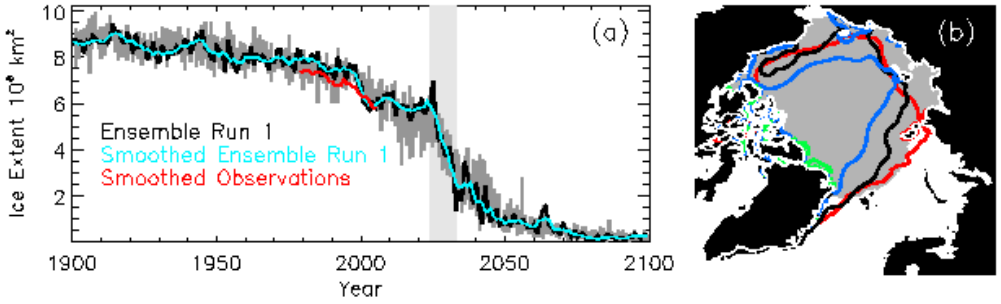

Figure 10: (a) Northern Hemisphere September sea ice extent for 20C3M and A1B simulations with the CCSM3 climate model. The black line shows ice extent from Run 1 of 6 CCSM3 simulations, the blue line is the five-year running mean of the black line, and the red line is the five-year running mean ice extent from observations. The range of extent values from the 6 CCSM3 simulations is in dark grey, and the light grey band indicates the abrupt sea ice loss event. (b) Averaged September sea ice edge, defined as the boundary between gridpoints with at least 50% sea ice fraction and gridpoints with less than 50% ice fraction. The black and red contours show the mean 1990s September ice edge for Run 1 and the observations, respectively. The blue contour is the Run 1 mean September edge for 2010 to 2019, and the green contour is the mean September edge for 2040 to 2049.

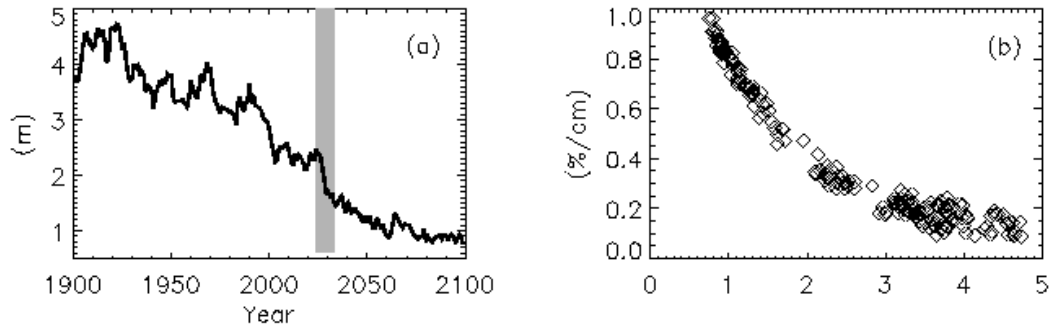

Figure 11: (a) The Arctic averaged March ice thickness and (b) the open water formation efficiency as a function of the March ice thickness for the simulation in figure 10. The open water formation efficiency is the open water formation, as a percent increase open water area, per centimeter of ice melt averaged over the melt season from May to August.

Values on the x-axis in panel (b) are in meters.

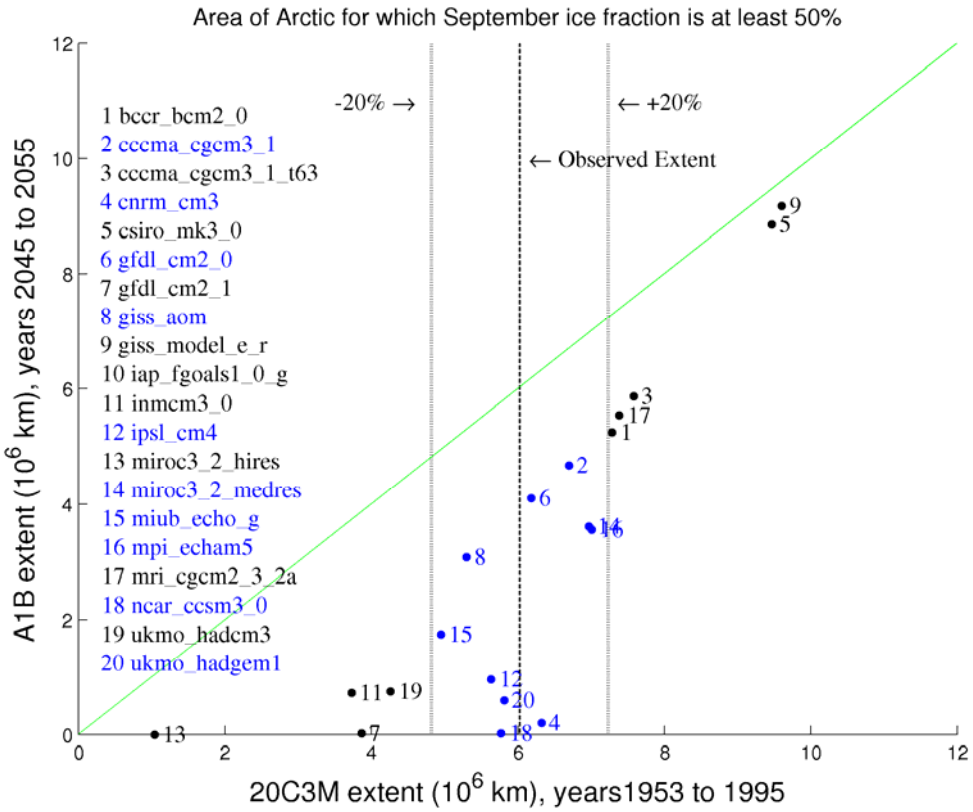

Figure 12: Climatological September sea ice extent in 20C3M and A1B simulations for the 20 models which contributed sea ice data to the IPCC AR4 archive.

Here sea ice extent is defined as the area of the Arctic in which the fractional ice coverage is at least 50%. The 20C3M climatology is calculated for the years 1953 to 1995, and the A1B climatology is calculated for 2045 to 2055. The vertical dashed line gives the 1953 to 1995 climatological September sea ice extent from the HadISST observational data set, and the dotted lines represent sea ice extent values 20% greater than and 20% less than the observed value. The green diagonal is the “no-change” line: a model with the same sea ice extent in the 20C3M and A1B climatologies would be represented by a dot lying on this line, and distance below the line represents the amount of loss between the two periods. Model acronyms are listed on the left side of the plot, and models with 20C3M extent within 20% of the observed value (i.e. lying between the two dotted lines) are colored blue. Model 10, iap_fgoals_0_g, is not displayed because its extent value is off the scale (about 19 million square kilometers, for 20C3M, 18 for A1B).